



One-dimensional  
simulation of fire  
injection heights

S. Strada et al.

# One-dimensional simulation of fire injection heights in contrasted meteorological scenarios with PRM and Meso-NH models

S. Strada<sup>1</sup>, S. R. Freitas<sup>2</sup>, C. Mari<sup>1</sup>, K. M. Longo<sup>2</sup>, and R. Paugam<sup>3</sup>

<sup>1</sup>Laboratoire d'Aérodologie, University of Toulouse and CNRS, UMR5560, Toulouse, France

<sup>2</sup>Center for Weather Forecasting and Climate Studies, INPE, Cachoeira Paulista, Brazil

<sup>3</sup>Department of Geography, King's College London, London, UK

Received: 12 December 2012 – Accepted: 17 January 2013 – Published: 6 February 2013

Correspondence to: S. Strada (susanna.strada@aero.obs-mip.fr), S. R. Freitas (saulo.freitas@cptec.inpe.br)

Published by Copernicus Publications on behalf of the European Geosciences Union.

Title Page

Abstract

Introduction

Conclusions

References

Tables

Figures



Back

Close

Full Screen / Esc

Printer-friendly Version

Interactive Discussion



## Abstract

Wild-fires release huge amounts of aerosol and hazardous trace gases in the atmosphere. The residence time and the dispersion of fire pollutants in the atmosphere can range from hours to days and from local to continental scales. These various scenarios highly depend on the injection height of smoke plumes. The altitude at which fire products are injected in the atmosphere is controlled by fire characteristics and meteorological conditions. Injection height however is still poorly accounted in chemistry transport models for which fires are sub-grid scale processes which need to be parametrised. Only recently, physically-based approaches for estimating the fire injection heights have been developed which consider both the convective updrafts induced by the release of fire sensible heat and the impact of background meteorological environment on the fire convection dynamics. In this work, two different models are used to simulate fire injection heights in contrasted meteorological scenarios: a Mediterranean arson fire and two Amazonian deforestation fires. A Eddy-Diffusivity/Mass-Flux approach, formerly developed to reproduce convective boundary layer in the non-hydrostatic meteorological model Meso-NH, is compared to the 1-D Plume Rise Model. For both models, radiosonde data and re-analyses from the European Center for Medium-Range Weather Forecasts (ECMWF) have been used as initial conditions to explore the sensitivity of the models responses to different meteorological forcings. The two models predict injection heights for the Mediterranean fire between 1.7 and 3.3 km with the Meso-NH/EDMF model systematically higher than the 1-D PRM model. Both models show a limited sensitivity to the meteorological forcings with a 20–30 % difference in the injection height between radiosondes and ECMWF data for this case. Injection heights calculated for the two Amazonian fires ranges from 5 to 6.5 km for the 1-D PRM model and from 2 to 4 km for the Meso-NH/EDMF model. The difference of smoke plume heights between the two models can reach 3–4 km. A large difference is obtained for the windy-wet Amazonian fire by the 1-D PRM model with a injection height 1.5 km higher when ECMWF re-analyses are used compared to the run with the radiosonde

## GMDD

6, 721–790, 2013

### One-dimensional simulation of fire injection heights

S. Strada et al.

Title Page

Abstract

Introduction

Conclusions

References

Tables

Figures

⏪

⏩

◀

▶

Back

Close

Full Screen / Esc

Printer-friendly Version

Interactive Discussion



forcing. For the Mediterranean case, both models forecast a plume injection height above the boundary layer, although there are evidences that this particular fire propagated near the surface, highlighting the current limitations of the two approaches.

## 1 Introduction

5 The spatial scale at which fire emissions may impact the chemical composition of the atmosphere depends on their dispersion, a process that is highly influenced by the height of injection of fire products. The smoke plume injection height is defined as the altitude at which the smoke particles are injected into the atmosphere before transport (Kahn et al., 2008). If fire pollutants stay trapped in the the Planetary Boundary Layer (PBL), their residence time can be shortened by removal processes that act  
10 more efficiently in the first layer of the atmosphere (Chatfield and Delany, 1990; Stein et al., 2009), and fire products may interact with urban and rural emissions with diverse consequences (e.g. Phuleria et al., 2005; Bytnerowicz et al., 2010). On the contrary, if fire emissions reach the free troposphere, their chemical lifetime increases and fire  
15 products are transported by faster winds that allow the spread of their effect on air quality from a local to a regional and occasionally intercontinental scale (Gidel, 1983; Saarikoski et al., 2007; Sofiev et al., 2008; Turquety et al., 2009; Dirksen et al., 2009).

The final height of injection of a smoke plume is a complex parameter to determine (i.e. to measure and to simulate). It is a result of dynamical interactions between the  
20 fire induced buoyant flows and the background environment (Freitas et al., 2006; Sofiev et al., 2012). It can change with time according to the fire propagation and evolution of the fire heat fluxes. Wildfires are intense sources of heat that is released in the atmosphere in the form of hot gases and water vapour. The contribution to sensible heat flux from wildland fires can not be neglected: values of sensible heat flux measured  
25 during on-field campaigns are nearly 3 orders of magnitude higher than natural fluxes (e.g. Clements et al., 2007; Silvani and Morandini, 2009). Under favourable meteorological conditions, fire-induced sensible heat flux has even the potential to enhance

## One-dimensional simulation of fire injection heights

S. Strada et al.

Title Page

Abstract

Introduction

Conclusions

References

Tables

Figures



Back

Close

Full Screen / Esc

Printer-friendly Version

Interactive Discussion



**One-dimensional  
simulation of fire  
injection heights**

S. Strada et al.

Title Page

Abstract

Introduction

Conclusions

References

Tables

Figures

⏪

⏩

◀

▶

Back

Close

Full Screen / Esc

Printer-friendly Version

Interactive Discussion



deep convection (so-called pyro-convection), leading to direct injection of smoke into the upper troposphere and lower stratosphere, as observed by Fromm et al. (2005) and Damoah et al. (2006), and as modelled by Trentmann et al. (2006). Smoke plumes are also masses of humid air with an increase of water vapour mixing ratio of nearly 30 % over the ambient air within the plume (Clements et al., 2006) due to the release of fuel and “combustion” moisture (Parmar et al., 2008). Also the plume-environment interaction plays an important role in the convection process. The hot fire plume interacts with the cooler surrounding air: this phenomenon can trigger turbulent eddies. Hence, fire-induced turbulence can efficiently mix environmental colder air into the fire plume, cooling the hot plume and reducing its upward movement (Freitas et al., 2006). Furthermore, turbulent motions can bring in the uprising plume some humid air from the environment leading to a gain of extra buoyancy from latent heat of condensation of the water vapour (Freitas et al., 2007). Additional buoyancy may also be gained if the rising haze plume reaches the Lifting Condensation Level (LCL), as already investigated for volcanic plume rise (Graf et al., 1999), beyond which water vapour begins to condense and latent heat is released. Studies on volcanic activities also showed the effect of strong horizontal winds on the final height of plumes (Bursik, 2001). The interaction between the plume and strong winds favours lateral entrainment of air, increasing the horizontal momentum. Particularly for small fires, this phenomenon results in plume bending and might reduce the updraft development because of losing the additional buoyancy from condensate water vapour (Freitas et al., 2010).

When run at very high resolution, atmospheric models can resolve explicitly convective transport and turbulent motions. Instead, at larger resolution (e.g. meso-scale), several types of atmospheric movements are sub-grid processes, and they are incorporated into atmospheric models through appropriate parametrisation schemes. As explained before, wild-fires can induce direct and rapid transport into the atmosphere, this process may have considerable impacts on the atmospheric dynamics and on pollutants distribution (Luderer et al., 2006; Tressol et al., 2008). Strong updrafts associated with fires are frequently ignored, or their impact is diluted, at the typical resolution of

**One-dimensional  
simulation of fire  
injection heights**

S. Strada et al.

Title Page

Abstract

Introduction

Conclusions

References

Tables

Figures



Back

Close

Full Screen / Esc

Printer-friendly Version

Interactive Discussion



large-scale models (Rio et al., 2010). Using three chemistry transport models (CTMs) driven by the same meteorology, Elguindi et al. (2010) performed sensitivity tests that underlined the role of low injection heights in the model's poor representation of the CO plumes. Singh et al. (2012) minimally succeeded in the attempts to simulate the complex interactions of fire emissions with urban and rural air. These peculiar interactions had been documented by airborne observations over California during large wildfires. Among shortcomings in air quality models that may contribute to the disagreement between observations and simulations, the authors cited uncertainties in plume-rise estimation.

Several studies were carried out using remote sensing data to investigate the height to which smoke plumes rise and the variability of this altitude due to fire characteristics. Labonne and Chevallier (2007) assessed the injection height of biomass burning plumes by analyzing the vertical distribution of aerosols, a good marker of fire emissions. They compared released data from the Cloud and Aerosol Lidar for Pathfinder Spaceborne Observations (CALIPSO) and the mixing layer top diagnosed by the European Center for Meteorological and Weather Forecasting (ECMWF); they concluded that biomass burning plumes were injected within the mixing layer. The same method was used by Amiridis et al. (2009); their results outlined that, under strong fire activity, the ECMWF diagnostic underestimates the BL height. Kahn et al. (2008) suggested to combine lidar observations with stereo imaging to support the modelling of smoke environmental impacts. Mazzone et al. (2007) utilized stereo imaging from the Terra Multi-angle Imaging Spectro-Radiometer (MISR) and the Moderate Resolution Imaging Spectro-radiometer (MODIS) data to locate fires and their smoke plumes, and they retrieved the injection height generated by fire buoyancy over a 4-month period. This work was extended by ValMartin et al. (2010) that analyzed a 5-yr record of MISR smoke plume injection heights over North America. Their analysis of plume heights indicated that 4–12 % of plumes from fires are injected above the BL; moreover, the MISR plume climatology exhibited larger summertime heights that, once correlated with MODIS Fire Radiative Power (FRP) measurements, seemed to be the result of

**One-dimensional simulation of fire injection heights**

S. Strada et al.

[Title Page](#)[Abstract](#)[Introduction](#)[Conclusions](#)[References](#)[Tables](#)[Figures](#)[Back](#)[Close](#)[Full Screen / Esc](#)[Printer-friendly Version](#)[Interactive Discussion](#)

higher fire intensity, likely due to most severe fire intensity during summer. The study of ValMartin et al. (2010) confirmed the conclusions of Sofiev et al. (2009) who showed, over a 2-yr period, the prevalence of fire injection heights within the BL over the US. Gonzi and Palmer (2010) used satellite observations of CO, a tracer of incomplete combustion, in order to estimate the vertical transport of surface fire emissions. Considering boreal and tropical wild-fires, they found that only 10–25 % of emissions are injected above the PBL. Guan et al. (2010) proposed a simple empirical method to identify biomass burning plume heights using the Aerosol Index (AI) measurements as determined by satellite instruments. The authors derived a best-fit relationship between AI and maximum plume height for young plumes that could help to validate the vertical placement of smoke plumes in CTMs.

In CTMs, vertical plume distributions have often been represented by means of empirical or arbitrary procedures such as uniformly distributing fire emissions within a few layers close to the surface up to a prescribed height which varies with the studied region (Liousse et al., 1996; Lamarque et al., 2003; Tressol et al., 2008). Other methodologies are to release fire products at different heights (Elguindi et al., 2010) or directly in the upper atmosphere when it comes to pyro-convection (Hyer et al., 2007). Some studies propose a link between plume height and fire intensity (Lavoué et al., 2000; Miranda, 2004; Hodzic et al., 2007). To improve these techniques, more physical and dynamical methods have been developed and implemented in meso-scale models with the scope to parametrise the plume lifting by taking into account fire characteristics and environmental conditions. A 1-D entrainment Plume Rise Model (1-D PRM) was presented by Freitas et al. (2006, 2007). It could be embedded in a host 3-D meso-scale or global model to simulate explicitly the convective transport mechanism associated with wild-fires and determine the final height where fire products, emitted during the flaming phase, would be released. This plume rise algorithm was implemented and successfully tested with the NCAR Community Atmosphere Model for modelling the transport of carbon monoxide (CO) released by Southern Africa biomass burning, showing significant improvements in the vertical distribution of CO (Guan et al., 2008). PRM was

# GMDD

6, 721–790, 2013

## One-dimensional simulation of fire injection heights

S. Strada et al.

Title Page

Abstract

Introduction

Conclusions

References

Tables

Figures



Back

Close

Full Screen / Esc

Printer-friendly Version

Interactive Discussion



coupled with the Coupled Aerosol and Tracer Transport model to the Brazilian develop-  
ments on the Regional Atmospheric Modeling System (CATT-BRAMS, Freitas et al.,  
2009; Longo et al., 2010). The model of Freitas et al. (2007) was also integrated in the  
WRF model with Chemistry (WRF-Chem) showing significant improvements in weather  
5 forecasting (Grell et al., 2011) and in the emissions transport and dispersion (Sessions  
et al., 2011). The study of pyro-convection was also addressed by the work of Rio et al.  
(2010) who, starting from the “thermal plume model” of Hourdin et al. (2002), proposed  
a “pyro-thermal plume model” based on a mixed Eddy Diffusivity/Mass Flux (EDMF)  
scheme for convective boundary layer plumes. In the EDMF parametrisation, the up-  
10 draft and the surrounding environment directly interact through local and non-local mix-  
ing, respectively associated with the turbulent transport and the mass-flux term; the  
methodology of the 1-D PRM model relies on the assumption that at rough resolution  
(grid-scale  $\sim 30$  to 100 km) fires do not have significant effects on the dynamics and  
the thermodynamics of the host model. The works of Freitas et al. (2010) and Rio et al.  
15 (2010) mark the current state of the art in the domain of atmosphere-wildfire interac-  
tion and they underline the challenge that remains when it comes to dealing with fire  
injection height. So far, these approaches have been applied and partially validated for  
some wild-fires occurred in different scenarios (boreal, Amazonian and African fires),  
some of which presented elevated injection heights. Recently, Sofiev et al. (2012) pro-  
20 posed a new methodology to evaluate the smoke-injection height from wildfires that is  
similar to existing Convective Available Potential Energy (CAPE) computations used for  
describing deep convection. The authors applied their methodology to remote-sensing  
data for about 2000 fire plumes in North America and Siberia. They also compared  
their diagnostic of the smoke-injection height with other methods, such as the MISR  
25 plume-top, Briggs’ plume-rise formulas, the 1-D PRM BUOYANT (Martin et al., 1997),  
and the prescribed injection height widely used in CTMs. Just selecting a part of the  
MISR data-set, Sofiev et al. (2012) showed a significant improvement in their diag-  
nostic compared with cited approaches. Moreover, in contrast to other approaches

(e.g. Freitas et al., 2010), they stated that the wind speed is unimportant for the wild fire plume height.

The main goal of the present study is to delve into the dynamics of strong updrafts associated with wild-fires, focusing on the main actors participating in the smoke plume rise process: heat fluxes (sensible and latent), turbulence and entrainment of ambient air. Moreover, this work aims to investigate the impact of weather conditions on fire evolution, taking into account different meteorological forcings. For this purpose, sensitivity analyses are designed to compare two approaches for predicting the fire injection height, once both numerical models operate with similar environmental and fire conditions. The Meso-NH model is used at a kilo-metric scale in a 1-D configuration to study a typical Mediterranean fire (Lançon-de-Provence 2005) and two deforestation fires burnt in 2002 in the Amazon basin under different meteorological conditions. The capacity of the EDMF scheme in Meso-NH (Pergaud et al., 2009) is here investigated related to strong convective processes associated with wild-fires. Results from the 1-D Meso-NH/EDMF model are compared to corresponding simulations generated by the 1-D PRM model of Freitas et al. (2010). For both models, radiosonde data and re-analyses from the ECMWF are used as initial conditions to explore the sensitivity of both models to different meteorological forcing.

The paper is organized as follows. Section 2 introduces the selected case studies, discussing differences in the atmospheric profiles between radiosondes and ECMWF re-analyses. Section 3 gives a brief description of the two 1-D models (Meso-NH/EDMF and PRM). In Sects. 4 and 5, simulation results are presented and discussed, after having defined an unifying metrics adopted for the comparison. Finally, conclusions are summarized in Sect. 6.

## 2 Data-sets selected for the inter-comparison

Three wild-fires have been selected as case studies for the comparison exercise and are described in this section: a Mediterranean arson fire and two Amazonian

## One-dimensional simulation of fire injection heights

S. Strada et al.

Title Page

Abstract

Introduction

Conclusions

References

Tables

Figures



Back

Close

Full Screen / Esc

Printer-friendly Version

Interactive Discussion



deforestation fires. These cases differ from one another in vegetation characteristics and in meteorological conditions, suggesting a different evolution of the smoke plume rise.

For each of the three scenarios, initial and boundary meteorological conditions are from radiosondes and operational re-analyses from the ECMWF. The difference in the initial atmospheric profile between a radiosonde and re-analysis field has consequences on the atmosphere that is simulated by the numerical model, leading to different behaviours for the fire plume.

Figure 1 shows the atmospheric conditions in the first kilometres for the Mediterranean fire. The vertical profiles of temperature, wind speed, potential temperature and water vapour mixing ratio are traced up to an height of 8 km for the radiosonde data (dashed line) and the ECMWF analysis (solid line). Data for the Amazonian fires are presented respectively in Figs. 2 and 3.

## 2.1 Lançon-de-Provence 2005

On 1 July 2005, an arson wild-fire broke out at about 07:40 UTC, 09:40 CEST (Center European Summer Time) to the east of Lançon-de-Provence (south-eastern France, 43.60° N, 5.20° E), threatening downwind inhabited areas and cultivated lands. At 12:00 UTC, on the burning area, firefighters measured a temperature of 26 °C, a wind speed of 46 kmh<sup>-1</sup>, a wind direction of 330° and a relative humidity of 20%. Documented favourable weather conditions led to the fire spreading easily. After 8 h of burning, the Lançon fire was put out and the burnt area estimated: nearly 626 ha, mainly covered by shrub-land and forest.

Twice a day (at 00:00 and at 12:00 UTC) a radiosonde is launched over Nîmes, a city located 63 km northwest away from Lançon-de-Provence (43° N, 4° E). Looking at radiosonde data measured on 1 July 2005 at 12:00 UTC (14:00 local time), temperatures decrease from 25 to ~ 0 °C in the first 5 km of the atmosphere (Fig. 1a). A well marked temperature inversion is observed at nearly 760 hPa, around 2.3 km; above this altitude the atmosphere becomes more stable as depicted by the positive slope of the potential

## One-dimensional simulation of fire injection heights

S. Strada et al.

Title Page

Abstract

Introduction

Conclusions

References

Tables

Figures

◀

▶

◀

▶

Back

Close

Full Screen / Esc

Printer-friendly Version

Interactive Discussion



## One-dimensional simulation of fire injection heights

S. Strada et al.

Title Page

Abstract

Introduction

Conclusions

References

Tables

Figures

◀

▶

◀

▶

Back

Close

Full Screen / Esc

Printer-friendly Version

Interactive Discussion



temperature trend (Fig. 1b). This last graphic highlights unstable conditions at the surface ( $\partial_z \theta < 0$ ), followed by a well developed mixed layer where  $\theta$  is constant: this is the typical convective boundary layer of a summer early afternoon. Figure 1c shows a dry CBL with water vapour mixing ratio that decreases from  $6.5 \text{ g kg}^{-1}$  at the surface to nearly  $1.0 \text{ g kg}^{-1}$  at 700 hPa. The layer above is moister, probably as a result of the radiosonde crossing a cloud; normally this “wet” layer would not interact with the fire plume since strong winds, together with a dry BL, may efficiently prevent fire plume rise, as pointed out by Trelles et al. (1999) and Freitas et al. (2007). Strong northwesterly winds blow over the region with speeds ranging from 8 to  $20 \text{ ms}^{-1}$  in the first 2 km of the atmosphere (Fig. 1d).

The Lançon-de-Provence fire constituted a benchmark for fire spread models (Fore-Fire and FARSITE, Balbi et al., 2009); moreover, the dynamics and the chemistry downwind of the Lançon fire were investigated by Strada et al. (2012).

## 2.2 Rondônia 2002

Rondônia is a state in Brazil located in the north-western part of the country and bordered Bolivia. Rondônia landscape underwent a rapid conversion between 1984 and 2002 after the opening of the BR-364 highway and the introduction of pasture in the 70s. With one of the fastest rate of tropical deforestation (Lovejoy, 1991), rain-forests have been soon replaced by agricultural and pasture lands by means of fires (de Barros Ferraz et al., 2005).

In 2002, during the burning season, two radiosondes were launched at 18:00 UTC (on 20 and 27 September) near a deforestation area in Rondônia ( $11.0^\circ \text{ S}$ ,  $60.0^\circ \text{ W}$ ). Radiosonde time, 18:00 UTC, is 14:00 local time when the diurnal cycle of Amazonian fires reaches its peak (Freitas et al., 2010) and convective structure are well developed (Chou et al., 2007). The selected days differ in wind intensity and atmospheric humidity, for this reason the considered case studies have been renamed as follows: the calm-dry case corresponds to 20 September 2002; the windy-wet case refers to 27 September 2002.

## One-dimensional simulation of fire injection heights

S. Strada et al.

Title Page

Abstract

Introduction

Conclusions

References

Tables

Figures

⏪

⏩

◀

▶

Back

Close

Full Screen / Esc

Printer-friendly Version

Interactive Discussion



Considering the radiosoundings:

- *Calm-dry case*. On 20 September 2002 temperatures pass from 35 to  $\sim 0^\circ\text{C}$  in the first 5 km of the atmosphere; a strong thermal inversion is observed at around 800 hPa,  $\sim 2\text{ km}$  (Fig. 2a). Below 800 hPa the potential temperature and the water vapour mixing ratio are constant in the daytime mixed layer; above the BL is capped by the stably stratified and drier free atmosphere, with  $r_v$  decreasing abruptly from 12 to  $3\text{ g kg}^{-1}$  (Fig. 2b, c). The wind speed accelerates in the first kilometres from 2 to  $4\text{ ms}^{-1}$ , then the speed decreases to  $1\text{ ms}^{-1}$  at 700 hPa, around 3 km (Fig. 2d). Analysing the zonal and the meridional wind, also a directional wind shear is identified in the first 3 km (not shown).
- *Windy-wet case*. On 27 September 2002 the radiosonde registers a weaker temperature inversion at lower levels (around 870 hPa,  $\sim 1.5\text{ km}$ , Fig. 3a). The height of the daytime mixed layer is nearly 1 km ( $\partial_z\theta \approx 0$ , Fig. 3b). Above, in the stable atmosphere,  $r_v$  decreases suddenly from 12 to  $9\text{ g kg}^{-1}$  (Fig. 3c). The wind speed increases with height up to an altitude of 2 km with a strong wind shear from 2 to  $6\text{ ms}^{-1}$  (Fig. 3d).

These two meteorological situations have already been chosen as case studies for other model comparisons (Freitas et al., 2007, 2010). Significant differences in ambient wind and humidity between the calm-dry and the windy-wet case will permit to better understand the role and the importance of environmental conditions on the smoke rise process, having selected the same fire characteristics for both cases.

## 2.3 Comparison between radiosondes and ECMWF analyses

### 2.3.1 Lançon-de-Provence 2005

The ECMWF analysis shows a weaker temperature inversion at a slightly lower altitude compared to the radiosounding: 800 hPa, around 1.8 km (Fig. 1a). The potential

temperature presents a less marked instability at the ground, followed by a mixed layer that stretches up to about 800 hPa (Fig. 1b). The trend of the water vapour mixing ratio describes a drier atmosphere at the ground-level and a moister one in the mixed layer, but in general the ECMWF atmosphere is drier compared to the one described by the radiosonde (Fig. 1c). In Fig. 1d the ECMWF wind speeds are quite similar in the first 1.5 km to those of the radiosonde, except for a relative maximum around 2 km of altitude.

### 2.3.2 Rondônia 2002

- *Calm-dry case.* A rapid inspection of the ECMWF vertical profiles showed a striking difference between the ECMWF and the radiosonde profiles. In the first 2 km the ECMWF atmosphere looks cooler, more stable, with a water vapour mixing ratio monotonically decreasing (Fig. 2a–c). Moreover, the ECMWF vertical profile is moister in the first kilometer, then it becomes drier. Between the ground surface and an altitude of 2 km, winds are  $2 \text{ ms}^{-1}$  weaker on the average if compared to the radiosonde atmosphere, in the layer above the magnitude relation inverts. Furthermore, the ECMWF profile shows a weaker wind shear.
- *Windy-wet case.* As for the calm-dry case, the ECMWF vertical profiles look very different compared to those traced using the radiosonde. In the first 2 km the ECMWF atmosphere is cooler, even of  $10^\circ\text{C}$  at the surface (Fig. 2a); moreover, it is more stable with potential temperature monotonically increasing with height, Fig. 2b. The water vapour mixing ratio decreases and the ECMWF atmosphere is highly moister than the radiosonde: at the inversion height the difference in water vapour mixing ratio equals  $6 \text{ g kg}^{-1}$  (Fig. 2c). Concerning wind speeds, the comparison is quite good for the windy-wet case (Fig. 2d).

Comparing the Lançon-de-Provence case study to the two Amazonian cases, it is worthy to note that the Amazon Basin offers a warmer, moister and less windy atmosphere for the fire starting.

## One-dimensional simulation of fire injection heights

S. Strada et al.

Title Page

Abstract

Introduction

Conclusions

References

Tables

Figures



Back

Close

Full Screen / Esc

Printer-friendly Version

Interactive Discussion



### 3 Description of the one-dimensional models

This section is mainly devoted to describe the numerical models that have been used and compared in the present work: the 1-D PRM and the Meso-NH/EDMF. Because of the computational efficiency of a 1-D model and the ability to isolate a column of atmosphere for study, a single column model (SCM) is an ideal environment in which to develop and test parametrisations (Randall et al., 1996).

#### 3.1 The Meso-NH 1-D/EDMF model

Meso-NH is a meteorological research model jointly developed by the Centre National de Recherche Météorologiques (Météo France) and the Centre National de Recherche Scientifique (Laboratoire d'Aérodologie) (Lafore et al., 1998). This numerical model was designed to simulate atmospheric motion at different scales (from the large meso down to the micro scale) using the non-hydrostatic assumption and the an-elastic approximation. Meso-NH has a standard three dimensional (3-D) configuration, however it is here run as a SCM, using version 4.8-4. In the present study, cloud micro-physical processes follow a two-moment scheme, using three water phases with five species of precipitating and non-precipitating liquid and solid water (Pinty and Jabouille, 1998). Turbulent motions are represented by the quasi-1-D scheme of Bougeault and Lacarrère (1989). The Eddy-Diffusivity/Kain-Fritschl parametrisation is utilized for representing shallow convection (see Sect. 3.1.2 for further information).

The used square grid-mesh has an horizontal resolution of 1 km and the vertical grid has 70 levels, with a level spacing stretching from 40 m near the ground to 600 m at higher altitude. The integration time is one hour with a time-step of one second. Due to the short duration (1 h) of the simulation, radiative processes are neglected (i.e. the downward radiative flux is put to zero) and the Coriolis parameter  $f$  is set to zero. The orography is not taken into account, depicting a flat domain.

Dynamical variables are initialized and constrained prescribing a stationary vertical profile (i.e. the initial and the final state of the atmosphere are the same). Two

GMDD

6, 721–790, 2013

## One-dimensional simulation of fire injection heights

S. Strada et al.

Title Page

Abstract

Introduction

Conclusions

References

Tables

Figures

◀

▶

◀

▶

Back

Close

Full Screen / Esc

Printer-friendly Version

Interactive Discussion



## One-dimensional simulation of fire injection heights

S. Strada et al.

Title Page

Abstract

Introduction

Conclusions

References

Tables

Figures

⏪

⏩

◀

▶

Back

Close

Full Screen / Esc

Printer-friendly Version

Interactive Discussion



different types of vertical profile are used: observational soundings recorded in the vicinity of the burnt area, on the day of the fire; and vertical profiles generated from operational re-analyses of the ECMWF, selecting the same UTC hour of the observational radiosonde and the nearest location to the radiosonde launch station. For the three scenarios, radiosondes and ECMWF re-analyses are available at same hours (12:00 UTC for Lançon and 18:00 UTC for the Rondonia fires) when the diurnal cycle of wild-fires is more pronounced (Hodzic et al., 2007; Freitas et al., 2009).

The Interactions Soil-Biosphere-Atmosphere scheme (ISBA, Noilhan and Planton, 1989) is used for parametrising exchanges between the atmosphere and natural or agricultural lands and provides surface energy fluxes to the atmosphere. In order to have the same contribution from the ground, in terms of fluxes, the same kind of vegetation cover has been chosen in Meso-NH for all three scenarios, imposing equal conditions for soil humidity and temperature. The selected cover type is cerrado; temperatures of the surface soil layer, the root zone soil layer and the deep soil layer have been set to 303.53 K; and soil water index (SWI) is zero for the surface soil layer and 0.2 for the root zone and the deep soil layer.

The fire forcing is activated through heat and scalar fluxes that are prescribed at the ground level in the Meso-NH model: Sect. 3.1.3 gives further details on this technique.

### 3.1.1 1-D Meso-NH general equations

A SCM is a stand-alone model that can be pictured as a single vertical array of grid-point cells placed at a specific geographical location. The column model prognostically calculates the evolution of the vertical structure of some variables based on physical parametrisations. In particular, in the 1-D Meso-NH prognostic variables are: latitudinal and longitudinal wind components ( $u$ ,  $v$ ), potential temperature ( $\theta$ ), water vapour ( $r_v$ ), cloud ( $r_c$ ) and rain water ( $r_r$ ) mixing ratios and turbulent kinetic energy (TKE,  $\bar{e}$ ).

The basic equations implemented in the 1-D Meso-NH are:

$$\frac{\partial \bar{u}}{\partial t} = \frac{\partial}{\partial z} \left( K_m \frac{\partial \overline{w'u'}}{\partial z} \right) - w_{ls} \frac{\partial \bar{u}}{\partial z} \quad (1)$$

$$\frac{\partial \bar{v}}{\partial t} = \frac{\partial}{\partial z} \left( K_m \frac{\partial \overline{w'v'}}{\partial z} \right) - w_{ls} \frac{\partial \bar{v}}{\partial z} \quad (2)$$

$$\frac{\partial \bar{\theta}}{\partial t} = \frac{\partial}{\partial z} \left( K_h \frac{\partial \overline{w'\theta'}}{\partial z} \right) - w_{ls} \frac{\partial \bar{\theta}}{\partial z} + Q_{\theta}^{diab} \quad (3)$$

$$\frac{\partial \bar{r}_j}{\partial t} = \frac{\partial}{\partial z} \left( K_h \frac{\partial \overline{w'r'_j}}{\partial z} \right) - w_{ls} \frac{\partial \bar{r}_j}{\partial z} + Q_{r_j}^{diab}; \quad j \in \{v, c, r\} \quad (4)$$

$$\frac{\partial \bar{e}}{\partial t} = \frac{\partial}{\partial z} \left( K_e \frac{\partial \bar{e}}{\partial z} \right) - w_{ls} \frac{\partial \bar{e}}{\partial z} + K_m \left[ \left( \frac{\partial u}{\partial z} \right)^2 + \left( \frac{\partial v}{\partial z} \right)^2 \right] + K_h \frac{g}{\theta_v} \overline{w'\theta'_v} - D. \quad (5)$$

Here the primed variables denote perturbations, bar refers to averaged variables. The parameter  $w_{ls}$  is the synoptic-scale vertical velocity,  $K_m$ ,  $K_h$  and  $K_e$  are the turbulent mixing coefficients for momentum, heat and TKE, respectively.  $Q_{\theta}^{diab}$  and  $Q_{q_j}^{diab}$  are the diabatic terms in the heat and humidity equations. The parameter  $g$  is the gravitational constant. The temporal evolution of  $\bar{e}$  depends on different terms that are, on the right side of Eq. (5), the turbulent transport by eddies, the vertical advection by large scale vertical flow, the shear production or loss term, the buoyancy production, and the dissipation rate of TKE, respectively.

To sum up, in the atmosphere of the SCM the active processes are: vertical advection, turbulent mixing and diabatic exchanges. The vertical velocity is handled as a diagnostic variable.

### 3.1.2 The EDMF parametrisation

Recently, a specific parametrisation for shallow convection in the boundary layer has been included in the Meso-NH research model. The new scheme takes into account the impact on the boundary layer dynamics of sub-grid strong convective updrafts generated by surface heating (i.e. dry thermals, Pergaud et al., 2009). The whole concept is based on a scale decomposition where the organized, non-local, strong updrafts are described by an advective Mass-Flux approach (second term on the right side of Eq. 6), whereas the remaining local turbulent field is represented by the Eddy-Diffusivity approach (Siebesma and Teixeira, 2000; Hourdin et al., 2002; Witek et al., 2011; first term on the right side of Eq. 6). As a consequence, the vertical turbulent flux of a conservative variable  $\phi$  is defined as

$$\overline{w'\phi'} = -K \frac{\partial \overline{\phi}}{\partial z} + \frac{M_u}{\rho} (\phi_u - \overline{\phi}), \quad (6)$$

where  $\rho$  is the air density,  $K$  is the turbulent eddy diffusivity coefficient for the variable  $\phi$ ,  $M_u$  is the convective mass flux in the updraft  $M_u = \rho a_u w_u$  ( $a_u$  is the updraft fractional area and  $w_u$  is the vertical velocity in the updraft),  $\overline{\phi}$  is the mean value and  $\phi_u$  is the updraft value of the variable  $\phi$ . In the following, the subscript u is always used for variables associated with the updraft whereas the subscript e refers to variables associated with the environment.

The basic idea of the EDMF approach is to depict dry thermals as towers of buoyant air rising from the surface and developing in a Convective Boundary Layer (CBL); these strong updrafts are not isolated but they interact with the surrounding environment through turbulent mixing that favours entrainment and detrainment of air masses between the convective parcel and its environment. Therefore, once the EDMF parametrisation is implemented in an atmospheric model, it allows a physical coupling between the updraft and the environmental air: the dynamics and the thermodynamics of both evolve due to a reciprocal influence.

## GMDD

6, 721–790, 2013

### One-dimensional simulation of fire injection heights

S. Strada et al.

Title Page

Abstract

Introduction

Conclusions

References

Tables

Figures

◀

▶

◀

▶

Back

Close

Full Screen / Esc

Printer-friendly Version

Interactive Discussion



The Mass Flux approach describes the evolution of updraft structures ensuring the mass balance through a diagnostic mass continuity equation:

$$\frac{1}{M_u} \frac{\partial M_u}{\partial z} = \varepsilon - \delta. \quad (7)$$

The mass-flux evolves along the vertical at a rate given by the difference between the entrainment  $\varepsilon$  and the detrainment  $\delta$  rate. The definition of entrainment/detrainment rates is the crucial point in EDMF parametrisation: it is at this level that the physical coupling between turbulent mixing and mass flux is done.

The mass-flux profile depends on the vertical velocity of the updraft, whose vertical evolution is affected in turn by a buoyancy term ( $B_u$ ) and a drag term where the entrainment of environmental air, namely lateral mixing, is accounted for:

$$w_u \frac{\partial w_u}{\partial z} = aB_u - b\varepsilon w_u. \quad (8)$$

The updraft buoyancy acceleration is evaluated related to the difference of virtual potential temperature  $\theta_v$  between the updraft and its environment, in the absence of phase change in water:  $B_u = g(\theta_{u,v} - \overline{\theta_v})/\overline{\theta_v}$ ; parameters  $a$  and  $b$  are set to one (Simpson and Wiggert, 1969). The vertical velocity Eq. (8) can be solved to find the top of the updraft imposing  $w_u \rightarrow 0$  as boundary condition. Moreover, independent solutions of Eqs. (7) and (8) permit to calculate the vertical variation of the updraft fractional area:

$$a_u = \frac{M_u}{\rho w_u}, \quad (9)$$

that is used to diagnose the cloud fraction, hence to define the sub-grid condensation scheme in the EDMF framework.

Hourdin et al. (2002) noticed a tilt effect on the thermal while introducing the drag effect of apparent wind in the equations for horizontal momentums. However, in the “pyrothermal plume model” of Rio et al. (2010), the momentum transport is not parametrised.

**One-dimensional simulation of fire injection heights**

S. Strada et al.

Title Page

Abstract

Introduction

Conclusions

References

Tables

Figures



Back

Close

Full Screen / Esc

Printer-friendly Version

Interactive Discussion



In the EDMF scheme a vertical non-local mixing of momentum is performed by taking into account the contribution of the Mass Flux approach on the horizontal momentum, in addition to the mixing already activated by the turbulent scheme. Hence, the updraft horizontal wind components evolve as

$$\frac{\partial u_u}{\partial z} = -\varepsilon(u_u - \bar{u}) + C_v \frac{\partial \bar{u}}{\partial z}, \quad (10)$$

$$\frac{\partial v_u}{\partial z} = -\varepsilon(v_u - \bar{v}) + C_u \frac{\partial \bar{v}}{\partial z}, \quad (11)$$

where  $C_u = C_v = 0.5$ ;  $u_u$  ( $v_u$ ) is the zonal (meridional) component of wind in the updraft;  $\bar{u}$  and  $\bar{v}$  are the zonal and meridional mean wind components, respectively.

As pointed out before, the definition of entrainment and detrainment rates characterizes the EDMF parametrisation. Pergaud et al. (2009) chose to draw the definition of lateral mass exchanges from the updraft buoyancy and vertical velocity. Both these parameters are pertinent in shallow convection as they control the mixing rate between the updraft (dry or moist) and its environment. For the dry case, the entrainment/detrainment rate is locally defined as an equilibrium between  $w_u$  and  $B_u$ :

$$\varepsilon_{\text{dry}}, \delta_{\text{dry}} \propto \frac{B_u}{w_u^2}, \quad (12)$$

For the moist portion of the updraft a different definition of lateral mass exchange is used. In Meso-NH, if the LCL is reached, lateral exchanges are computed using the entraining/detraining plume model of Kain and Fritsch (1990) that considers the cloud radius.

Finally, the scheme initialization is given at the surface ( $z_{\text{grd}}$ ) computing the mass-flux as follows:

$$M_u(z_{\text{grd}}) \propto \rho \left( \frac{g}{\theta_{v,\text{ref}}} \overline{w' \theta'_{v,s}} L_{\text{up}} \right)^{1/3}, \quad (13)$$

## One-dimensional simulation of fire injection heights

S. Strada et al.

Title Page

Abstract

Introduction

Conclusions

References

Tables

Figures

◀

▶

◀

▶

Back

Close

Full Screen / Esc

Printer-friendly Version

Interactive Discussion



where  $g$  is the acceleration of gravity,  $\theta_v$  is the virtual potential temperature  $\overline{w'\theta'_{v,s}}$  is the surface buoyancy flux,  $L_{up}$  is the upward mixing length corresponding to the distance that a parcel leaving the ground travels due to buoyancy, as defined by Bougeault and Lacarrère (1989). From the Turbulent Kinetic Energy  $e$  at the ground, the vertical velocity of the updraft at the surface results:

$$w_u^2(z_{grd}) = \frac{2}{3}e(z_{grd}). \quad (14)$$

### 3.1.3 Fire forcing in Meso-NH

At the horizontal resolution selected for the Meso-NH simulation (1 km), wild-fires are considered as sub-grid processes in the atmospheric model, hence their effect on the atmosphere needs to be parametrise. An off-line coupling is activated between the fire and the atmospheric model (i.e with no feedback of the atmosphere on the fire) by adapting to a 1-D configuration the methodology of Strada et al. (2012) developed for a 3-D simulation. Working in a simple 1-D scenario permits to assess the strength of the fire forcing on the atmospheric dynamics and to discriminate fire effects from other phenomena.

The coupling method consists in providing the burning area ( $S_b$ ) contained in each Meso-NH grid cell ( $S_{mnh}$ ) every 2 min, assuming the wild-fire as stationary. At each atmospheric time-step, the surface scheme ISBA accomplishes the fire-atmosphere coupling by computing total wildfire contribution to latent and sensible heat fluxes, taking into account a nominal flux and the surface ratio between the Meso-NH and the total burnt area. Finally, calculated fluxes are taken as inputs at the surface level in the atmospheric model. A step function tunes the starting of the fire during the first five minutes, as done in the 1-D PRM model (Freitas et al., 2007).

The sensible heat flux  $\Phi_S$ ,  $\text{kWm}^{-2}$ , is computed as

$$\Phi_S = \phi_s \cdot C \cdot \frac{S_b}{S_{mnh}}. \quad (15)$$

## GMDD

6, 721–790, 2013

### One-dimensional simulation of fire injection heights

S. Strada et al.

Title Page

Abstract

Introduction

Conclusions

References

Tables

Figures

◀

▶

◀

▶

Back

Close

Full Screen / Esc

Printer-friendly Version

Interactive Discussion



## One-dimensional simulation of fire injection heights

S. Strada et al.

Title Page

Abstract

Introduction

Conclusions

References

Tables

Figures

◀

▶

◀

▶

Back

Close

Full Screen / Esc

Printer-friendly Version

Interactive Discussion



The nominal value  $\phi_S$  does not separate radiative from convective energy; hence, the multiplication by a reducing factor,  $C$ , is necessary to select the percent of total energy effectively available to plume convection. The  $C$  parameter ranges from 0.4 to 0.8 depending on fire characteristics and ambient conditions; in order to compare results from the Meso-NH and the 1-D PRM model, the same value selected by Freitas et al. (2010) has been chosen:  $C = 0.55$  (from McCarter and Broido, 1965). The surface  $S_{\text{mnh}}$  measures 100 ha. A constant value is imposed for the burnt area,  $S_b = 3.35$  ha, by taking the mean burnt area simulated by a fire propagation model as described in (Strada et al., 2012). This condition insures that during the simulation time step from 12:00 to 13:00, the effective burnt area is 100 ha. The same value is used for the Amazonian fires for which no information on the time evolution of fire burnt area is available.

The latent heat flux  $\Phi_L$ ,  $\text{kgm}^{-2}\text{s}^{-1}$ , is calculated as in the 1-D PRM model:

$$\Phi_L = \frac{\Phi_S}{E_m} \cdot \left[ \frac{m}{100} + \text{EF}_{\text{H}_2\text{O}} \right]. \quad (16)$$

The computed sensible heat flux multiplies the heat content  $E_m$  ( $\text{MJkg}^{-1}$ ) by the sum of fuel moisture  $m$  (%) and H<sub>2</sub>O emission factor (combustion moisture, in  $\text{kgkg}^{-1}$ ).

A fire tracer is emitted and its flux ( $\text{gm}^{-2}\text{s}^{-1}$ ) is defined as follows:

$$\Phi_{\text{fire}} = \frac{E_{\text{fire}}}{S_{\text{mnh}} \cdot \tau}, \quad (17)$$

where the fire emission  $E_{\text{fire}}$  (in g) are integrated on the Meso-NH grid-mesh, on a period of 2 min,  $\tau$ . The fire emission is obtained through the equation of Seiler and Crutzen (1980):

$$E_{\text{fire}} = S_b \cdot \text{FL} \cdot \beta \cdot \text{EF}_{\text{fire}}, \quad (18)$$

where FL ( $\text{kgm}^{-2}$ ) is the fuel loading,  $\beta$  (%) is the burning efficiency of the above-ground biomass, and  $\text{EF}_{\text{fire}}$  ( $\text{gkg}^{-1}$ ) is the emission factor for the fire tracer. From Miranda et al. (2008), FL and  $\beta$  for shrub-lands are  $1.00 \text{ kgm}^{-2}$  and 80 %, respectively.

The fire tracer is handled as a  $\text{PM}_{10}$  aerosol ( $\text{EF}_{\text{fire}} = 10 \text{g kg}^{-1}$ ) with no mass (i.e. deposition velocity equals  $0 \text{m s}^{-1}$ ).

Table 1 summarizes the fire characteristics used for simulating different fire episodes (for references: Freitas et al., 2007; Silvani and Morandini, 2009; Miranda et al., 2008).

The same fuel moisture is selected for Mediterranean and Amazonian vegetation; this choice is justified by the necessity to limit the number of varying parameters between different scenarios. Moreover, recent discussions on the role of fuel moisture state a minor importance of this parameter on fire evolution compared to contributions from the environment in terms of humid air (Luderer et al., 2006; Strada et al., 2012).

### 3.2 The 1-D PRM model

Starting from the simple 1-D time-dependent cloud resolving model of Latham (1994), Freitas et al. (2006) proposed a plume rise model for simulating explicitly strong up-drafts associated with vegetation fires and for, finally, predicting the fire injection height. The model governing equation for vertical motion includes the entrainment of environmental air in the plume, the difference of temperature between the environment and the plume, the upward drag of condensate water vapour, the pyro-convection (i.e. release of latent heat when forming ice), and the effect of horizontal ambient wind (Freitas et al., 2010). The scope of the 1-D PRM model is to make a parametrisation available to 3-D meso-scale or global models in order to describe the sub-grid convective transport associated with wild-fires, taking into account fire features, and to better forecast dispersion of fire products (aerosols and trace gases).

The 1-D plume rise model can be embedded in each column of a large-scale atmospheric-chemistry transport model. The coupling between the 1-D PRM and the host model relies on the assumption that at rough resolution (grid-scale  $\sim 30$  to  $100 \text{km}$ ) fires do not have significant effects on the dynamics and the thermodynamics of the host model. In this way, the 3-D model passes the environmental large-scale conditions to the 1-D PRM model for initializing and constraining it at the boundaries, under

## One-dimensional simulation of fire injection heights

S. Strada et al.

Title Page

Abstract

Introduction

Conclusions

References

Tables

Figures



Back

Close

Full Screen / Esc

Printer-friendly Version

Interactive Discussion



the hypothesis of a stationary atmosphere. Once the convective energy flux of the fire and the plume radius have been selected, the 1-D PRM model resolves explicitly the vertical extent of the fire plume. For each biome type two values for the fire heat flux are given: a lower and an upper; therefore, the 1-D PRM model computes a lower and an upper injection height. These two results are returned to the host model that homogeneously releases fire tracers emitted during the flaming phase in the vertical range delimited by the lower and the upper height. The 1-D PRM model can be run independently with initial values from a radiosonde.

The fire heat flux is converted into the available convective energy flux  $E$  (in  $\text{kW m}^{-2}$ ) multiplying it by the reducing factor  $C = 0.55$ , already defined for the Meso-NH model (Sect. 3.1.3). Hence, the buoyancy flux ( $\text{m}^4 \text{s}^{-3}$ ) generated at the surface by the fire source is calculated using the following expression:

$$F = \frac{g\mathcal{R}}{c_p P_e} E R^2, \quad (19)$$

where  $\mathcal{R}$  is the ideal gas constant ( $\text{kg}^{-1} \text{K}^{-1}$ ),  $c_p$  is the specific heat capacity at constant pressure ( $\text{J kg}^{-1} \text{K}^{-1}$ ),  $P_e$  is the ambient surface pressure (hPa) and  $R$  is the plume radius (m), computed at the surface by assuming the burning area as a circle.

Buoyancy triggers the vertical velocity ( $w_{f,0}$ ) and the temperature excess ( $T_f - T_e$ ) of the in-cloud air parcels at a virtual altitude (Morton et al., 1956):

$$w_{f,0} = \frac{5}{6\alpha} \left( \frac{0.9\alpha F}{z_v} \right)^{1/3}, \quad (20)$$

$$\frac{\Delta\rho_0}{\rho_{e,0}} = \frac{5}{6\alpha} \frac{F}{g} \frac{z_v^{-5/3}}{(0.9\alpha F)^{1/3}}, \quad (21)$$

$$T_f = \frac{T_e}{1 - \frac{\Delta\rho}{\rho}}, \quad (22)$$

One-dimensional simulation of fire injection heights

S. Strada et al.

Title Page

Abstract

Introduction

Conclusions

References

Tables

Figures

⏪

⏩

◀

▶

Back

Close

Full Screen / Esc

Printer-friendly Version

Interactive Discussion



where  $\alpha = 0.05$ ,  $z_v = (5/6)\alpha^{-1}R$  is the virtual boundary height, and  $\Delta\rho_0$  is the density difference between the in-cloud air parcels and environmental air at the surface. The surface water vapour excess is calculated in the same way that is reported for the Meso-NH model (Eq. 16). The heating rate increases following a step function during the first five minutes of the simulation. The time integration is fixed to one hour, as for Meso-NH, even if the steady state is typically reached within 50 min (Freitas et al., 2007). Hereafter, the subscript f is used to identify variables associated with the center of mass of the rising plume.

The 1-D PRM model depicts the evolution of the plume utilizing advection equations for the vertical velocity  $w_f$ , the temperature  $T_f$ , the water phases parameters  $r_{f,v}$ ,  $r_{f,c}$  and  $r_{f,ice-rain}$ , the horizontal velocity of the center of mass of the plume at level  $z$  ( $U_f$ ) and the plume radius  $R$ . The governing prognostic equations are:

$$\frac{\partial w_f}{\partial t} + w_f \frac{\partial w_f}{\partial z} = \frac{1}{1+\gamma} g B_f - (\varepsilon_{f,lat} + \varepsilon_{f,dyn}) w_f \quad (23)$$

$$\frac{\partial T_f}{\partial t} + w_f \frac{\partial T_f}{\partial z} = -w_f \frac{g}{c_f} - (\varepsilon_{f,lat} + \varepsilon_{f,dyn})(T_f - T_e) + \left( \frac{\partial T_f}{\partial t} \right)_{\mu p} \quad (24)$$

$$\frac{\partial r_{v,f}}{\partial t} + w_f \frac{\partial r_{v,f}}{\partial z} = -(\varepsilon_{f,lat} + \varepsilon_{f,dyn})(r_{v,f} - r_{v,e}) + \left( \frac{\partial r_{v,f}}{\partial t} \right)_{\mu p} \quad (25)$$

$$\frac{\partial r_{c,f}}{\partial t} + w_f \frac{\partial r_{c,f}}{\partial z} = -(\varepsilon_{f,lat} + \varepsilon_{f,dyn}) r_{c,f} + \left( \frac{\partial r_{c,f}}{\partial t} \right)_{\mu p} \quad (26)$$

$$\frac{\partial r_{j,f}}{\partial t} + w_f \frac{\partial r_{j,f}}{\partial z} = -(\varepsilon_{f,lat} + \varepsilon_{f,dyn}) r_{j,f} + \left( \frac{\partial r_{j,f}}{\partial t} \right)_{\mu p} + \text{sedim}_j; \quad j \in \{\text{ice, rain}\} \quad (27)$$

$$\frac{\partial U_f}{\partial t} + w_f \frac{\partial U_f}{\partial z} = -(\varepsilon_{f,lat} + \varepsilon_{f,dyn})(U_f - U_e) \quad (28)$$

$$\frac{\partial R}{\partial t} + w_f \frac{\partial R}{\partial z} = \left( \frac{3}{5} \varepsilon_{f,lat} + \frac{1}{2} \varepsilon_{f,dyn} \right) R, \quad (29)$$

One-dimensional simulation of fire injection heights

S. Strada et al.

Title Page

Abstract

Introduction

Conclusions

References

Tables

Figures

◀

▶

◀

▶

Back

Close

Full Screen / Esc

Printer-friendly Version

Interactive Discussion



where in Eq. (23)  $\gamma = 0.5$  compensates for the neglect of non-hydrostatic pressure perturbations (Simpson and Wiggert, 1969) and  $B_f$  is the buoyancy term. Compared to the EDMF parametrisation, in the PRM the ice phase, that drives pyro-convection, is taken into account. Furthermore, the buoyancy term includes directly the downward drag of non-precipitating hydrometeors (ice, cloud droplet and hail) and its definition is related to the virtual temperature  $T_v$ . Index  $\mu_p$  denotes the tendencies from cloud microphysics (Freitas et al., 2007). The plume top is identified by means of the in-cloud vertical velocity: when  $w_f$  is less than  $1 \text{ ms}^{-1}$  over a certain time, the steady state solution is attained and the top of the plume is given by the model.

In the new version of the 1-D PRM model two terms of entrainment have been defined, the classical lateral entrainment

$$\varepsilon_{f,\text{lat}} = \frac{2\alpha}{R} |w_f|, \quad (30)$$

and the “dynamic entrainment”

$$\varepsilon_{f,\text{dyn}} = \frac{2}{\pi R} (U_e - U_f). \quad (31)$$

This additional entrainment term expresses some physical effects on the plume that are enhanced by strong horizontal winds: the reduction of the in-plume vertical velocity ( $-\varepsilon_{f,\text{dyn}} w_p$ ), the decrease of the buoyancy term due to the loss of temperature excess ( $-\varepsilon_{f,\text{dyn}} [T_f - T_e]$ ) and the gain of horizontal velocity of the plume ( $\varepsilon_{f,\text{dyn}} [U_f - U_e]^2$ ) (Freitas et al., 2010).

In the last update of the 1-D PRM model, Freitas et al. (2010) introduced the Vertical Mass Distribution (VMD) to mathematically define an injection layer. The VMD provides a probability vertical mass distribution as a function of the simulated vertical velocity profile ( $w_f$ ). Premising that the main detrainment mass layer of cumulus convection is situated close to the cloud top, two levels are defined:  $z_i$  where  $w_f$  starts to decrease, and  $z_f$  where  $w_f$  is less than  $1 \text{ ms}^{-1}$ . The area included among is the upper half part of

One-dimensional simulation of fire injection heights

S. Strada et al.

Title Page

Abstract

Introduction

Conclusions

References

Tables

Figures



Back

Close

Full Screen / Esc

Printer-friendly Version

Interactive Discussion



the cumulus (plume). Afterwards, a parabolic function of the height  $z$  with roots  $z_i$  and  $z_f$  is defined. Finally, the function is normalized to 1 in the interval  $[z_i, z_f]$ .

It is important to highlight that the 1-D PRM model is not a SCM as the 1-D Meso-NH model. In PRM, the evolution of the vertical structure of the prognostic meteorological variables within the plume does not impact the dynamics and the thermodynamics of the surrounding (grid-scale) environment in the host model. The 1-D PRM model is the adaptation of a cloud resolving model, a numerical model conceived to resolve cloud-scale circulation; therefore, it integrates over the whole cloud-area. Once adapted to the study of fire plume, the cloud-area is identified with the burnt area. In the present study, the prescribed burning area corresponds to the whole area that burned during the time integration: 100 ha (Sect. 3.1.3).

## 4 Results and analysis

In this section, results obtained from the 1-D Meso-NH/EDMF and the 1-D PRM model are presented and analysed, firstly by defining a unifying metrics for the discussion of results (Sect. 4.1), afterward by examining separately the three wild-fire episodes (Sect. 4.2).

### 4.1 Definition of the metrics used for the comparison

The EDMF and PRM schemes present a strong conceptual difference. The EDMF parametrisation is tightly coupled to the evolution of the grid-scale dynamics and thermodynamics variables through the entrainment and detrainment processes. The EDMF approach recalculates a new vertical distribution of state variables including tracers at each time step of the model in response to the perturbed grid-scale environment. The 1-D PRM model follows a diagnostic approach, in response to a stationary environment, where the fire plume rising stops evolving when all energy from fire characteristics and stationary atmospheric conditions has been used. This conceptual difference

## One-dimensional simulation of fire injection heights

S. Strada et al.

Title Page

Abstract

Introduction

Conclusions

References

Tables

Figures



Back

Close

Full Screen / Esc

Printer-friendly Version

Interactive Discussion



entails a distinct method for simulating fire episodes: Meso-NH/EDMF burnt 100 ha in 1 h, while PRM burnt 100 ha for 1 h. Due to these conceptual differences, the time evolution of the injection height during the simulation time can not be compared between the two models. Rather, the discussion focuses on the injection heights at the end of the simulated time.

Table 2 gathers all variables that have been selected for the comparison between the two numerical models. Regarding these variables, it is important to define a common metrics. First of all, the Meso-NH model distinguishes between grid and updraft variables when the EDMF scheme is activated, otherwise only grid variables are available in the model; on the contrary, the PRM variables only refer to the updraft system. Figure 4 shows several parameters from the 1-D PRM model for the Lançon-de-Provence case. Figure 6 presents the time evolution of the vertical profiles of parameters for the 1-D Meso-NH simulation on the same case. These two figures will be used to illustrate the variables chosen for the comparison study.

- *Water vapour mixing ratio.* In both models,  $r_v$  is expressed in  $\text{g kg}^{-1}$ . In the PRM model, the water vapour mixing ratio is representative of the updraft ( $r_{v,t}$ ). For the Meso-NH model,  $r_{v,\text{env}}$  is the value in the environment. It is worth noting that the net contribution of wild-fires is to increase the humidity of the air near the detrainment levels (Figs. 4a and 6a). This moist enrichment of the atmosphere determines the elevation of the vertical level where  $r_v$  reduces and keeps constant (i.e. higher cloud base compared with ambient conditions Luderer et al., 2009) along the total integration time (see Figs. 4a and 6a).
- *Updraft vertical velocity.* In both models, vertical velocity is expressed in  $\text{m s}^{-1}$ , but different trends are identified due to different theoretical definitions. In the PRM model  $w_f$  is initialised at the surface (Eq. 20) by the buoyancy flux and decreases along the vertical (Fig. 4b); whereas in the Meso-NH model,  $w_u$  is a prognostic variable whose trend strongly depends on the updraft fraction  $a_u$  and the updraft

**One-dimensional simulation of fire injection heights**

S. Strada et al.

Title Page

Abstract

Introduction

Conclusions

References

Tables

Figures

◀

▶

◀

▶

Back

Close

Full Screen / Esc

Printer-friendly Version

Interactive Discussion



mass flux  $M_u$  behaviour:

$$w_u = \frac{M_u}{\rho a_u},$$

where  $a_u$  increases near the surface then diminishes along the vertical, while  $M_u$  maximises in the mixing layer (Fig. 6b).

- *Buoyancy*. The buoyancy acceleration is given in  $\text{ms}^{-2}$ , and it shows similar trends and values for both models (Figs. 4c and 6c). In general, the buoyancy acceleration slightly increases near the surface, where the heat source is active and feeds the rising of the in-cloud parcels, then it reduces until the sign inversion, when downdraft movements start. Near the cloud top, equilibrium is attained (buoyancy equals zero).
- *Turbulent parameters*. Updraft turbulent fluxes ( $\langle w'_u \theta'_u \rangle$  in  $\text{Kms}^{-1}$ , and  $\langle w'_u r'_{v,u} \rangle$  in  $\text{kgkg}^{-1} \text{ms}^{-1}$ ) and turbulent kinetic energy (in  $\text{m}^2 \text{s}^{-2}$ ) are only available for the Meso-NH model. The updraft turbulent kinetic sensible heat flux  $\langle w'_u \theta'_u \rangle$  represents the buoyancy source in the equation of the TKE (Eq. 5), therefore its trend nearly resembles that of buoyancy with a deeper increment near the surface heating (in the first kilometres of the atmosphere), followed by a faster decrease until the equilibrium is reached ( $\langle w'_u \theta'_u \rangle = 0$ , Fig. 6d). The temporal evolution of the updraft turbulent kinetic latent heat flux  $\langle w'_u r'_{v,u} \rangle$  shows a clear rising of the altitude at which the maximum is placed that finally matches with the location of maximal fluctuations of  $w_u$  and  $r_{v,\text{env}}$  in the upper part of the updraft (Fig. 6e).
- *Entrainment*. In Meso-NH, the entrainment rate  $\varepsilon_u$  is measured in  $\text{m}^{-1}$  (Eq. 12), whereas in the PRM model the two entrainment rates are both expressed in  $\text{s}^{-1}$  (Eqs. 30 and 31). For consistency, the entrainment fluxes of Meso-NH/EDMF ( $E_u = \varepsilon M_u$ , in  $\text{kgm}^{-3} \text{s}^{-1}$ ) are multiplied by the density of dry air ( $\rho$ , in  $\text{kgm}^{-3}$ ) in order to have a common metrics for the entrainment coefficients:  $\text{s}^{-1}$ . Although

## GMDD

6, 721–790, 2013

### One-dimensional simulation of fire injection heights

S. Strada et al.

Title Page

Abstract

Introduction

Conclusions

References

Tables

Figures



Back

Close

Full Screen / Esc

Printer-friendly Version

Interactive Discussion



## One-dimensional simulation of fire injection heights

S. Strada et al.

Title Page

Abstract

Introduction

Conclusions

References

Tables

Figures



Back

Close

Full Screen / Esc

Printer-friendly Version

Interactive Discussion



the definitions are slightly different, the lateral entrainment  $\varepsilon_{f,\text{lat}}$  of the PRM model (Eq. 30) can be compared to the entrainment rate in the EDMF scheme of Meso-NH, Eq. (12): their values and exponential trends are similar (Figs. 4f and 6f). In the PRM model,  $\varepsilon_{f,\text{lat}}$  has the same value at the surface through the whole set of simulations (between  $0.3 \times 10^{-2}$  and  $0.4 \times 10^{-2} \text{ s}^{-1}$ ), likely due to the huge burnt area (100 ha) that homogenizes the existing differences in terms of fire forcings between Mediterranean and tropical fires (role of the plume radius in Eqs. 19 and 30). In the Meso-NH model, the entrainment coefficient at the surface has a constant value of  $0.2 \times 10^{-2} \text{ s}^{-1}$  that is comparable with the lateral entrainment in PRM.

Concerning the dynamic entrainment  $\varepsilon_{f,\text{dyn}}$  of the PRM model (Eq. 31) a similar parameter is not available in the Meso-NH model, therefore we decided to show in the following the sum of the two entrainment terms in order to illustrate the total entrainment of ambient air that feed, or slow down, the rising of the fire plume in the PRM model. Changes in the vertical profile of  $\varepsilon_{f,\text{dyn}}$  are driven by the fluctuations of environmental wind. In Fig. 4d,  $\varepsilon_{f,\text{dyn}}$  has a quasi monotonic decrease compatible with the wind profile in Fig. 1d.

- *Detrainment.* As done for the entrainment rate, the Meso-NH detrainment coefficient  $\delta_u$  is converted from  $\text{m}^{-1}$  to  $\text{s}^{-1}$ . The trend of  $\delta_u$  points out the coexistence of entrainment/detrainment in the CBL that both feed the vertical evolution of the mass flux; when  $\varepsilon_u$  goes to zero,  $\delta_u$  maximises (Fig. 6f). In Meso-NH, we define the detrainment zone (or injection layer) as the vertical range where  $\delta_u$  maximises. The injection height is the altitude at which the detrainment is maximal. Since the PRM model does not have a detrainment rate or zone among its output variables, the Meso-NH detrainment layer is compared to the vertical range enclosed by the VMD in the 1-D PRM simulations. The injection height is identified as the altitude where VMD maximises in the PRM model (Fig. 4f). In the graphics, the injection layers are compared by overlaying the VMD for the steady

## One-dimensional simulation of fire injection heights

S. Strada et al.

Title Page

Abstract

Introduction

Conclusions

References

Tables

Figures



Back

Close

Full Screen / Esc

Printer-friendly Version

Interactive Discussion



state solution of the PRM (dot filled area) on the plot of the Meso-NH detrainment rate (Fig. 6f). The mathematical definition of the VMD implies that the PRM model vents the fire products (from the flaming phase) away from the surface inducing a depletion of the lower levels of the atmosphere in terms of fire pollutants (Fig. 4f) which are no more available for turbulent mixing. In the Meso-NH/EDMF model, a part of the released fire tracer is mixed in the first kilometres of the atmosphere by the turbulence, the rest is vertically transported by the thermal plume (Fig. 6f).

- *Scalar*. As explained before (Sect. 3.1.3), a fire tracer is released in the Meso-NH simulations. Its mixing ratio is normalized by its maximal value at each temporal session. In general, once released at the surface, the fire tracer is partly transported high in the atmosphere and released near the top of the updraft (Fig. 6d) showing a characteristic “C-shape” profile.

## 4.2 Comparison of fire forced simulations

Table 3 recapitulates simulations that are here shown: RSOU stands for simulations forced by radiosonde data, ECMWF means that the meteorological forcing is taken from the ECMWF re-analyses. For the 1-D PRM model, only results obtained considering the environmental wind drag are presented since the difference between a simulation with the wind effect on/off was already discussed in the work of Freitas et al. (2010). The top of the fire plume as predicted by the PRM is illustrated on all graphics by an horizontal solid line, the horizontal dashed line refers to the plume top when the environmental wind effect is off in the PRM model.

For the 1-D PRM model, the vertical profiles obtained after 10 min of simulation are drawn with a dashed line, while the solid line depicts the attained steady state solution. Results from the 1-D Meso-NH model are presented at the temporal session of the PRM model steady state solution (dashed line) and at the end of the simulation (after 60 min, solid line).

## 4.3 Lançon 2005 wild-fire

### 4.3.1 1-D PRM results

Using the radiosounding of Nîmes as meteorological forcing, the 1-D PRM model predicts a plume top near 2.5 km including the environmental wind effect (Fig. 4b); looking at the VMD, the main injection layer is localized between 1 and 2.5 km and it maximises near 1.7 km (Fig. 4f). This steady state solution is obtained after around 20 min. Above 1.5 km of altitude,  $r_{v,f}$  records a gain of  $1 \text{ gkg}^{-1}$  between the first output (after 10 min) and the steady state solution (Fig. 4a). This increase in  $r_{v,f}$  documents a growth of humidity inside the fire plume that come from combustion itself (fuel and combustion moisture) and from the entrainment of ambient air.

Forcing the 1-D PRM model by the ECMWF re-analyses, the forecast plume top is located at 3 km (wind on) after nearly 20 min of simulation. The main injection layer reaches out nearly 1.5 km, from 1.3 to 3 km, with its maximum attained around 2.2 km (Fig. 5c). Compared with values obtained using the radiosonde forcing, the plume top is 500 m higher, the injection layer has the same width with an injection height 700 m higher than the RSOU case. Diverse factors may lead to these differences. As observed in Sect. 2, the radiosounding has a stronger temperature inversion than the ECMWF atmospheric profile, an atmospheric parameter that may efficiently control the injection height of the fire plume, preventing it from reaching higher altitudes (Trentmann et al., 2003). Moreover, the radiosonde measured a stronger wind velocity at the surface: this results in a quasi-doubled dynamic entrainment ( $e_{f,dyn} = 0.011 \text{ s}^{-1}$  in the RSOU case versus  $e_{f,dyn} = 0.006 \text{ s}^{-1}$  using the ECMWF forcing, not shown), and in a faster decrease of  $B_f$  and  $w_f$  (not shown for the ECMWF case). In the first kilometres of the atmosphere, in the ECMWF forced simulation,  $B_f$  even increases before starting to diminish (Fig. 4c versus Fig. 5a). The weaker wind drag in the ECMWF simulation has a consequence also on  $r_{v,f}$ ; since the fire plume can rise higher and faster in the ECMWF case, the growth of water vapour mixing ratio within the plume begins higher

## GMDD

6, 721–790, 2013

### One-dimensional simulation of fire injection heights

S. Strada et al.

Title Page

Abstract

Introduction

Conclusions

References

Tables

Figures

◀

▶

◀

▶

Back

Close

Full Screen / Esc

Printer-friendly Version

Interactive Discussion



than the radiosonde case and it is even more significant: 3 km above the surface  $r_{v,f}$  increases of  $3 \text{ g kg}^{-1}$  during 10 min (not shown).

### 4.3.2 1-D Meso-NH/EDMF results

When forced by the radiosounding of Nîmes, after 60 min of simulation, the 1-D Meso-NH/EDMF model simulates an updraft that has its top near 3.8 km (Fig. 6b). This altitude is comparable to the plume top predicted by the 1-D PRM model without the wind drag (3.5 km, horizontal dashed line on Fig. 6b). The detrainment zone is localized between 2.7 and 3.7 km (Fig. 6f), above the turbulent mixing stops to be active (Fig. 6d–e), and the detrainment maximises at 3.3 km. The final injection height as predicted by Meso-NH is 1.6 km higher than the value simulated by the 1-D PRM model using the RSOU forcing. This difference reduces ( $< 1 \text{ km}$ ) when we consider Meso-NH outputs after 20 min (PRM steady state solution). The illustrated dissimilarity can be ascribed to the weaker entrainment rate at the surface in the 1-D Meso-NH/EDMF model:  $\varepsilon_u = 0.002 \text{ s}^{-1}$  (Fig. 6f, positive values) against  $0.004 \text{ s}^{-1}$  for  $\varepsilon_{f,lat}$  in the respective 1-D PRM simulation (Fig. 4e). The Meso-NH updraft entrains less environmental air, therefore the cooling of the fire plume due to the mixing with ambient air is weaker resulting in a more convective updraft than the PRM plume. The same case study has been simulated by the 1-D Meso-NH without the EDMF parametrisation. The vertical spread is weaker because only the local mixing due to turbulence is considered: after 60 min, the TKE falls to zero at 3.1 km (Fig. 7b), as a consequence the fire tracer is not transported higher than this level (Fig. 7c). Even if a detrainment zone is not defined for this case, the relative VMD overlays the normalized vertical profile of the tracer mixing ratio just below the level where the diminution of the scalar mixing ratio becomes faster (2.6 km on Fig. 7c). The comparison between Fig. 6 (with EDMF) and Fig. 7 (without EDMF) shows the contribution of the mass flux approach which transport efficiently the boundary layer products to the higher altitudes.

## One-dimensional simulation of fire injection heights

S. Strada et al.

Title Page

Abstract

Introduction

Conclusions

References

Tables

Figures



Back

Close

Full Screen / Esc

Printer-friendly Version

Interactive Discussion



**One-dimensional  
simulation of fire  
injection heights**

S. Strada et al.

[Title Page](#)[Abstract](#)[Introduction](#)[Conclusions](#)[References](#)[Tables](#)[Figures](#)[⏪](#)[⏩](#)[◀](#)[▶](#)[Back](#)[Close](#)[Full Screen / Esc](#)[Printer-friendly Version](#)[Interactive Discussion](#)

Once forced by the ECMWF profile, at the end of the simulation, the updraft in the 1-D Meso-NH/EDMF model stops rising at around 3.2 km, and it detrains between 2.2 and 3.2 km with its maximum at 2.7 km (Fig. 8b). In this case, the comparison of the injection layer between the two models is better than for the RSOU forcing with a difference of only 500 m. For both models, the buoyancy acceleration starts reducing around 2 km of altitude (Fig. 8c versus Fig. 5a). The Meso-NH entrainment rate (Fig. 5b) is still the half than the PRM lateral entrainment (not shown); considering the total entrainment for the PRM model (Fig. 5b), Meso-NH nearly entrains one fourth of the ambient air compared to PRM (Fig. 5b). As before, the Meso-NH simulation without the EDMF scheme predicts a lower injection height (2.5 km after 60 min of integration time, not shown).

### 4.3.3 General comments

The 1-D PRM model predicts a higher injection height (by nearly 500 m) when it is forced by the ECMWF re-analysis because this meteorological forcing has weaker winds at the surface than the radiosonde. Using the 1-D Meso-NH/EDMF model, the result is opposite with nearly the same variability (600 m): the final injection height is higher for the RSOU case rather than the ECMWF case. The 1-D PRM would prescribe to a host CTM a fire injection height that represents a fire plume escaping the PBL. The measurements recorded downwind of the Lançon fire by the air quality monitoring network gave evidences of a fire plume kept in contact with the surface (Strada et al., 2012). When the EDMF parametrisation is not activated, the 1-D Meso-NH model predicts a lower plume top that is more comparable with the air quality observations reported for the Lançon fire in the work of Strada et al. (2012).

## 4.4 Rondonia 2002 wild-fire: calm-dry case

### 4.4.1 1-D PRM results

Once initialised by the radiosonde, the 1-D PRM predicts a plume top at 6.9 km (wind on) with a maximum of 4% of mass around 5 km and the main injection layer comprised between 3.3 and 6.9 km (Fig. 9c). This maximum is substantially lower than the 9% maximum obtained for the Lançon-de-Provence fire but the mass is distributed in a deeper layer than the Mediterranean case. The 1-D PRM steady state solution is obtained after around 30 min. At the surface, the buoyancy acceleration is  $0.03 \text{ ms}^{-2}$  stronger than for the Lançon fire (Fig. 9a). In Eq. (19) the convective energy flux  $E$  has diminished and the plume radius  $R$  keeps the same, therefore this difference can only be attributed to the lower ambient surface pressure  $P_e$  recorded in Rondônia. The dynamic entrainment is critically reduced compared to the Lançon case, leading to a reduction in the total entrainment (Fig. 9b). This is due to the non negligible variation in the ambient wind speed between the Mediterranean and the Amazonian atmospheric background (Sect. 2; Fig. 1 versus Fig. 2).

The 1-D PRM simulation forced with the ECMWF profile has a 700 m lower plume top (6.2 km, when including the wind drag) after around 40 min, and the injection layer is 600 m less deeper (from 3 to 6 km) with a maximum of 5% of mass around 4.8 km (Fig. 10c). At 1 km of altitude, the dynamic entrainment maximises using both forcings but with different values:  $0.3 \times 10^{-2} \text{ s}^{-1}$  for the RSOU case,  $0.1 \times 10^{-2} \text{ s}^{-1}$  for the ECMWF case. The influence of this dissimilar contribution is evident on the vertical profile of the total entrainment that decreases quasi monotonically along the vertical (Fig. 10b) compared to the more contrasted profile of the RSOU case (Fig. 9b). These trends reflect contrasts in terms of wind speed between the two forcings as highlighted in Sect. 2.

## GMDD

6, 721–790, 2013

### One-dimensional simulation of fire injection heights

S. Strada et al.

Title Page

Abstract

Introduction

Conclusions

References

Tables

Figures

⏪

⏩

◀

▶

Back

Close

Full Screen / Esc

Printer-friendly Version

Interactive Discussion



#### 4.4.2 1-D Meso-NH/EDMF results

The 1-D Meso-NH/EDMF simulation forced by the radiosounding reproduces an updraft top at 4.5 km. The detrainment zone is localized between 3 and 4.5 km, just overlaying the lower one third of the PRM injection layer (Fig. 11b). The injection height is 1.5 km lower than the value predicted by the 1-D PRM model. Although the well developed daytime mixed layer (Fig. 2b–c) and the surface heating associated with the fire, the buoyancy acceleration at the surface is nearly the half of the same parameter in the PRM model (Fig. 11a versus Fig. 9a). In the Meso-NH model, the influence of the ambient surface pressure seems not to be accounted for as observed for the 1-D PRM model.

Using the ECMWF forcing, the convective updraft in the 1-D Meso-NH/EDMF model rises up to around 4.5 km and it detrains between 2.2 and 3.5 km, maximising at 2.7 km (Fig. 12b). Also in this case, the comparison of the injection layer is unsatisfactory with a gap of around 2 km. The less turbulent atmospheric background reproduced by the ECMWF re-analyses (Fig. 2b–c) determines weaker turbulent kinetic heat fluxes than the Meso-NH simulation forced by the radiosounding (not shown).

#### 4.4.3 General comments

In contrast with general conclusions drawn for the Lançon fire, the 1-D PRM model predicts a higher injection height when forced by the radiosounding: even if the radiosonde recorded a stronger wind speed at the surface than the ECMWF re-analyses (hence a stronger dynamic entrainment), a stronger buoyancy acceleration is produced at the surface. Using the 1-D Meso-NH/EDMF model, the updraft stops rising at nearly the same altitude (4.5 km) for both forcings, while the detrainment zone and its maximum are located at different levels: 800 m higher when the environment is more turbulent (RSOU forcing). Concerning the comparison of the fire injection height as predicted by the two numerical models, the result is unsatisfactory: the Meso-NH/EDMF model is

GMDD

6, 721–790, 2013

### One-dimensional simulation of fire injection heights

S. Strada et al.

Title Page

Abstract

Introduction

Conclusions

References

Tables

Figures



Back

Close

Full Screen / Esc

Printer-friendly Version

Interactive Discussion



between 1.1 and 1.5 km lower than the PRM model. The main injection layers predicted by the two models partly overlay only for the case study initialised by the radiosounding.

## 4.5 Rondonia 2002 wild-fire: windy-wet case

### 4.5.1 1-D PRM results

5 Forced by the radiosonde, the 1-D PRM model simulates a plume top at 6.7 km (wind on) after around 50 min (steady state solution). The main injection layer is localized between 3.2 and 6.7 km and the injection height is around 5 km (Fig. 13c). The dynamic entrainment is  $0.1 \times 10^2 \text{ s}^{-1}$  stronger than the calm-dry case implying a similar discrepancy in the total entrainment (Fig. 13b versus Fig. 9b). At the surface, the buoyancy acceleration is about  $0.06 \text{ m s}^{-2}$  (Fig. 13a), slightly smaller than the Rondônia calm-dry case forced by the radiosounding (Fig. 9a).

10 In Fig. 14, the 1-D PRM simulation initialised by the ECMWF profile has a fire plume that rises up to 8.9 km (wind on) after the whole integration time (60 min). The meteorological scenario prescribed by the ECMWF profile offers favourable conditions for the plume rise: weak ambient winds (lower values for the total entrainment in Fig. 14b versus Fig. 13b) and high humidity in the air (Fig. 3c). The main injection layer reaches out 4.7 km, from 4.2 to 8.9 km, and 3 % of mass are injected at 6.5 km (Fig. 14c).

### 4.5.2 1-D Meso-NH/EDMF results

20 When forced by the radiosounding, the 1-D Meso-NH/EDMF model simulates an up-draft top at 4.5 km (15). Once again, the 1-D Meso-NH/EDMF plume top is notably lower than the one predicted by the 1-D PRM model using the radiosonde. The detrainment zone is localized between 2.5 and 4.5 km and it shows two maxima: at 3 and 4.1 km (Fig. 15b). The higher maximum and the associated detrainment overlays the lower half injection layer simulated by the respective 1-D PRM simulation.

## One-dimensional simulation of fire injection heights

S. Strada et al.

Title Page

Abstract

Introduction

Conclusions

References

Tables

Figures



Back

Close

Full Screen / Esc

Printer-friendly Version

Interactive Discussion



Figure 14 shows the results of the 1-D Meso-NH/EDMF forced by the ECMWF profile. The updraft top is located at 5 km. The detrainment process presents two main zones of activity: a stronger one at 2 km, a weaker one at 4 km (Fig. 14b). This feature influences the vertical profile of the scalar mixing ratio: above the first detrainment zone, the fire tracer is rapidly transported along the vertical up to 5 km (Fig. 14c). The presence of two detrainment zones and of a deeper vertical transport above the turbulent mixing layer document the role of the mass flux approach in the EDMF scheme. The mass flux term is responsible for non-local mixing that feeds the convective tower along the whole column. Although the detrainment zone stretches from 1.6 to 4.8 km, it does not overlay the vertical range of the respective VMD (Fig. 14b).

### 4.5.3 General comments

Regarding the PRM model, there is a difference of 1.5 km between the RSOU and the ECMWF case. This gap confirms the sensitivity of the model of Freitas et al. (2010) to the humidity and the wind pattern of the meteorological background: the ECMWF profiles show an atmosphere moister and less windy than the radiosounding (Fig. 3c, d). As observed for the calm-dry case, the Meso-NH/EDMF results do not record sensible variations, probably due to intrinsic limitations of the EDMF scheme, as it will be discussed in the following. The 1-D Meso-NH/EDMF model is not able to rise higher than 5 km, therefore the comparison with the 1-D PRM model is less satisfactory than for the calm-dry case. As for the calm-dry case, the comparison between the two numerical models is unsatisfactory, slightly better when using the radiosonde as meteorological forcing rather than the ECMWF re-analyses.

## 5 General discussion

In this section differences between the two approaches and the sensitivity to the meteorological forcing are discussed.

Figure 17 summarizes the injection heights and layers as predicted by the PRM and the Meso-NH/EDMF models for the three documented fire cases. Looking at this graphic, at first glance an outstanding difference is observed between the Mediterranean (Lançon 2005) and the Amazonian wild-fires (Rondônia 2002): although the fire-induced heat fluxes for the Mediterranean case have higher values than the Amazonian ones (Table 1), the windy and dry meteorological conditions of the Mediterranean Basin efficiently constrain the vertical development of the fire plume. This sensitivity is evident for the PRM model where the Mediterranean fire has an injection height that is 3–4 km lower than the Amazonian values, and the Mediterranean injection layer is nearly the half of those obtained for the Amazonian cases. The difference Mediterranean/Amazon is less definite for the Meso-NH/EDMF model that predicts fire injection heights in a range between 2 and 4 km, with a quite similar width of the injection layer (except for the Rondônia windy-wet case where two well distinct detrainment zones are observed).

The kind of meteorological forcing also influences the evolution of the convective updrafts. For the 1-D PRM, the injection height records a variation in a range between 500 m and 1.5 km for the same wild-fire, whereas the extent of the injection layer is quite similar for both meteorological forcings, except for the Rondônia windy-wet case where the main injection layer is 1.2 km wider using the ECMWF re-analyses rather than the radiosounding. The identified variabilities for the PRM model are highly influenced by the intensity of the ambient wind speed that determines, in turn, the intensity of the dynamic entrainment that governs the effectiveness of the wind drag; the humidity of the ambient air also plays an important role since, once moist air mixes with the updraft, the net result is to lighten the rising plume ( $\rho_{\text{dry}} < \rho_{\text{moist}}$ , e.g. Fig. 13 versus Fig. 14). For the 1-D Meso-NH/EDMF model, the level of maximum detrainment can vary between 500 m and 1 km between the two forcings. The 1-D Meso-NH/EDMF model is partly influenced by the atmospheric conditions in terms of turbulence that locally feed the turbulent flux of conservative variables (Eq. 6): the less turbulent environment for the Amazonian cases depicted by the ECMWF re-analysed (Figs. 2b, c and 3b, c) leads to

**One-dimensional  
simulation of fire  
injection heights**

S. Strada et al.

Title Page

Abstract

Introduction

Conclusions

References

Tables

Figures



Back

Close

Full Screen / Esc

Printer-friendly Version

Interactive Discussion



## One-dimensional simulation of fire injection heights

S. Strada et al.

Title Page

Abstract

Introduction

Conclusions

References

Tables

Figures



Back

Close

Full Screen / Esc

Printer-friendly Version

Interactive Discussion



lower injection heights. However, significant values observed for the updraft turbulent kinetic latent heat flux in the Rondônia calm-dry case do not lead to higher injection heights compared to other results. This model response is coherent with the thesis of Luderer et al. (2009) who state that the fire-released latent heat is of much lesser importance than the fire-released sensible heat.

Comparing results from the two numerical models, the Meso-NH/EDMF model simulates 0.5–1 km higher injection heights for the Mediterranean wild-fire, and 1.5–3.5 km lower values for the Amazonian cases. These gaps can be ascribed to the different intensity of the entrainment of ambient air in the two approaches. The Meso-NH model takes into account only the lateral entrainment, while the PRM model includes the effect of ambient wind among the environmental factors that may feed the lateral mixing of the rising plume. In the PRM model, this approach results in a total entrainment coefficient at the surface that is always the double of the Meso-NH value. As a consequences, the in-cloud parcels mix more efficiently with the ambient air in the PRM frame; hence, if the surrounding atmosphere is dry and windy (as for the Mediterranean fire), the net result is a drag force, while a humid and less windy atmosphere can feed the rising of the plume by triggering the pyro-convection (as for the Amazonian fires). These conclusions state the important role of ambient wind on the fire plume rise in contrast with the recent work of Sofiev et al. (2012). Both models used a total burnt area of 100 ha that burned in 1 h for Meso-NH, while for 1 h for PRM. This distinct design of simulations implied different fire fluxes at the surface for the two models with Meso-NH receiving 1/30 of the fire fluxes prescribed at the surface in PRM. In spite of this, the Meso-NH response is not systematically lower than PRM diagnostic.

For the Lançon fire, the two models simulate a fire injection height above the PBL, in contrast with the existing observations for the Lançon fire (Strada et al., 2012). For the Amazonian fires, there exist considerable differences between the two models. In particular, the 1-D Meso-NH/EDMF model simulates the injection heights in the lower half of the troposphere, below the zero isothermal (at about 5 km). This is an intrinsic limitation of the current version of EDMF in Meso-NH. The EDMF parametrisation was

## GMDD

6, 721–790, 2013

## One-dimensional simulation of fire injection heights

S. Strada et al.

Title Page

Abstract

Introduction

Conclusions

References

Tables

Figures



Back

Close

Full Screen / Esc

Printer-friendly Version

Interactive Discussion



implemented in the Meso-NH model to reproduce strato-cumulus clouds. Its design implies some important features that strongly limit the vertical evolution of the updraft: (1) the altitude of the zero-isothermal is a vertical limit in the rising of the updraft, (2) the ice phase is not yet activated, and (3) the cloud layer can not exceed a fixed 3 km extent. Similarly, Rio et al. (2010) discussed the use of the EDMF scheme in configurations, such as wild-fire episodes, for which this parametrisation has not been initially developed for, possibly leading to deep convection.

In general, it is important to underline the intrinsic limitations of the design that has been chosen for the present study. The choice of a 1 km horizontal grid-mesh was justified by the aim to study the vertical evolution of a fire plume in the same configuration of the Lançon-de-Provence 2005 case study (Strada et al., 2012). However, kilometric horizontal resolutions are intermediate scales for turbulence movements where these processes are not mainly resolved neither entirely parametrised. Honnert et al. (2011) investigated the behaviour of atmospheric models at intermediate scales (the so called “Terra Incognita” of the turbulence, Wyngaard, 2004) and they identified some misleading results of atmospheric models due to the presence of too many resolved movements, when the turbulence scheme parametrises the subgrid thermal, or an overestimation of the subgrid part, when a mass-flux scheme is introduced. Concerning the PRM model, a burnt area that measures 100 ha induces a strong decrease of the entrainment of ambient air (see Eqs. 30 and 31), hence it leads to a fire plume that rises fast in the atmosphere and does not mix properly with the surrounding air. Utilizing radiosondes to force the PRM model a difference of only 200 m is observed between the calm-dry and the windy-wet case. While forcing the PRM model by the same radiosoundings and using a burnt area of 10 ha, Freitas et al. (2010) observed a difference of nearly 1 km in terms of injection height between the calm-dry and the windy-wet case; such a significant difference was not observed when the authors considered a burnt area of 50 ha. In addition, at 1 km scale, the hypothesis of the grid size environmental air not impacted by the fire becomes questionable in the PRM model

since the horizontal scale is comparable with the horizontal scale of global and meso-scale models.

## 6 Conclusions and perspectives

When modelling wild-fires, the height of injection of fire products has a crucial importance for determining the distance and the direction the smoke will travel (Guan et al., 2010), and also for understanding interactions between fire emissions and urban pollution (Singh et al., 2012). The parameter of the fire injection height highlights the tight link that exists between the dynamics and the chemistry of a wild-fire: it depends on fire characteristics and meteorological conditions, and it determines the chemistry that will act on the fire plume and on the environmental air. Nowadays, several studies have been carried out to define a database of seasonally and regionally diverse plume heights in order to prescribe, or just validate, the fire injection height in CTMs (Labonne and Chevallier, 2007; ValMartin et al., 2010; Gonzi and Palmer, 2010; Guan et al., 2010). Furthermore, some physical approaches have been developed to predict the fire plume rise, these go from simple (Miranda, 2004; Hodzic et al., 2007) to more complex schemes such as the plume rise models (Freitas et al., 2010; Sofiev et al., 2012) or EDMF approaches (Pergaud et al., 2009; Rio et al., 2010).

In this work, sensitivity tests have been realised to compare the fire plume top predicted by the 1-D PRM and the 1-D Meso-NH/EDMF models. Three wild-fires have been chosen: a Mediterranean arson fire and two deforestation Amazonian fires. They distinguish from one another in terms of fire features and meteorological scenarios. Moreover, for each case, two meteorological forcings have been used to initialise each model: a radiosounding and a vertical profile taken from ECMWF re-analyses.

The predicted injection heights showed considerable differences from one model to the other regarding the kind of fire and, for a given model, between ECMWF and radiosounding forcings. A definite sensitivity to the type of fire is observed with predicted injection heights strongly driven by distinct meteorological conditions in the Mediter-

## One-dimensional simulation of fire injection heights

S. Strada et al.

Title Page

Abstract

Introduction

Conclusions

References

Tables

Figures



Back

Close

Full Screen / Esc

Printer-friendly Version

Interactive Discussion





deep convection. These developments are expected to significantly improve the accuracy of Meso-NH. Moreover, sensitivity tests have to be run on more documented fire episodes (e.g. the Quinault fire; Trentmann et al., 2003; Freitas et al., 2007), and at resolutions higher than kilometric horizontal scales in order to study the behaviour of Meso-NH when the atmospheric dynamics is fully resolved. Regarding the 1-D Plume Rise Model, perspectives rely on the numerical coupling between the model and the FRP information provided by MODIS, though first studies (ValMartin et al., 2012) show that the model input are difficult to constrain with the current accuracy of the available data (i.e. MISR, BL estimation). However such a development is attractive, as this evolution of PRM could take advantage of the collaborative project about Monitoring Atmospheric Composition and Climate (MACC II) in the frame of which FRP observations from MODIS are assimilated in the Global Fire Assimilation System (GFAS, Kaiser et al., 2012). The coupling between the PRM model and satellite observations (e.g. FRP) would permit to provide to PRM more accurate information concerning fire characteristics. This technique could improve PRM predictions of fire injection heights that are passed to chemical transport models.

*Acknowledgements.* This work has been partially supported by the French National Agency (ANR) in the frame of its COSINUS program (IDEA, ANR-09-COSI-006). The work was also funded by the University of Toulouse III (ATUPS scholarship) and by the GMAI (Group Modeling of the Atmosphere and its Interfaces) group of Karla Maria Longo at the National Institute for Space Research (INPE).



The publication of this article is financed by CNRS-INSU.

One-dimensional simulation of fire injection heights

S. Strada et al.

Title Page

Abstract

Introduction

Conclusions

References

Tables

Figures



Back

Close

Full Screen / Esc

Printer-friendly Version

Interactive Discussion



## References

- Amiridis, V., Giannakaki, E., Balis, D., Pytharoulis, I., Zanis, P., Melas, D., and Zerefos, C.: Injection height of smoke from biomass burning in Eastern Europe by the synergy of satellite active and passive remote sensing, in: Proc. 8th International Symposium on Tropospheric Profiling, edited by: Apituley, A., Russchenberg, H. W. J., and Monna, W. A. A., Delft, Netherlands, 18–23 October 2009. 725
- Balbi, J. H., Morandini, F., Silvani, X., Filippi, J. B., and Rinieri, F.: A physical model for wildland fires, *Combust. Flame*, 156, 2217–2230, 2009. 730
- Bougeault, P. and Lacarrère, P.: Parameterization of orography-induced turbulence in a meso-beta-scale model, *Mon. Rea. Rev.*, 117, 1872–1890, 1989. 733, 739
- Bursik, M.: Effect of wind on the rise height of volcanic plumes, *Geophys. Res. Lett.*, 28, 3621–3624, doi:10.1029/2001GL013393, 2001. 724
- Bytnerowicz, A., Cayan, D., Riggan, P., Schilling, S., Dawson, P., Tyree, M., Wolden, L., Tisell, R., and Preisler, H.: Analysis of the effects of combustion emissions and Santa Ana winds on ambient ozone during the October 2007 southern California wildfires, *Atmos. Environ.*, 44, 678–687, 2010. 723
- Chatfield, R. and Delany, A.: Convection links biomass burning to increased tropical ozone: however, models will tend to overpredict  $O_3$ , *J. Geophys. Res.*, 95, 18473–18488, doi:10.1029/JD095iD11p18473 1990. 723
- Chou, S. C., Marengo, J., Dereczynski, C. P., Waldheim, P. V., and Manzi, A. O.: Comparison of CPTEC GCM and Eta Model results with observational data from the Rondonia LBA reference site, Brazil, *J. Meteor. Soc. Japan*, 85A, 25–42, 2007. 730
- Clements, C. B., Potter, B. E., and Zhong, S.: In situ measurements of water vapor, heat, and  $CO_2$  fluxes within a prescribed grass fire, *Int. J. Wildland Fire*, 15, 1369–1382, doi:10.1071/WF09009, 2006. 724
- Clements, C. B., Zhong, S., Goodrick, S., Li, J., Potter, B. E., Bian, X., Heilman, W. E., Charney, J. J., Perna, R., Jang, M., Lee, D., Patel, M., Street, S., and Aumann, G.: Observing the dynamics of wildland grass fires: fireflux – a field validation experiment, *Bull. Am. Meteorol. Soc.*, 88, 1369–1382, 2007. 723
- Damoah, R., Spichtinger, N., Servranckx, R., Fromm, M., Eloranta, E. W., Razenkov, I. A., James, P., Shulski, M., Forster, C., and Stohl, A.: A case study of pyro-convection using trans-

GMDD

6, 721–790, 2013

### One-dimensional simulation of fire injection heights

S. Strada et al.

Title Page

Abstract

Introduction

Conclusions

References

Tables

Figures

◀

▶

◀

▶

Back

Close

Full Screen / Esc

Printer-friendly Version

Interactive Discussion



## One-dimensional simulation of fire injection heights

S. Strada et al.

Title Page

Abstract

Introduction

Conclusions

References

Tables

Figures



Back

Close

Full Screen / Esc

Printer-friendly Version

Interactive Discussion



port model and remote sensing data, *Atmos. Chem. Phys.*, 6, 173–185, doi:10.5194/acp-6-173-2006, 2006. 724

de Barros Ferraz, S. F., Vettorazzi, C. A., Theobald, D. M., and Ballester, M. V. R.: Landscape dynamics of Amazonian deforestation between 1984 and 2002 in central Rondônia, Brazil: assessment and future scenarios, *Forest Ecol. Manag.*, 204, 69–85, 2005. 730

Dirksen, R. J., Boersma, B. K. F., de Laat, J., Stammes, P., van der Werf, G. R., Martin, M. V., and Kelder, H. M.: An aerosol boomerang: rapid around-the-world transport of smoke from the December 2006 Australian forest fires observed from space, *J. Geophys. Res.*, 114, 148–227, doi:10.1029/2009JD012360, 2009. 723

Elguindi, N., Clark, H., Ordóñez, C., Thouret, V., Flemming, J., Stein, O., Huijnen, V., Moinat, P., Inness, A., Peuch, V.-H., Stohl, A., Turquety, S., Athier, G., Cammas, J.-P., and Schultz, M.: Current status of the ability of the GEMS/MACC models to reproduce the tropospheric CO vertical distribution as measured by MOZAIC, *Geosci. Model Dev.*, 3, 501–518, doi:10.5194/gmd-3-501-2010, 2010. 725, 726

Freitas, S. R., Longo, K. M., and Andreae, M. O.: Impact of including the plume rise of vegetation fires in numerical simulations of associated atmospheric pollutants, *Geophys. Res. Lett.*, 33, L17808, doi:10.1029/2006GL026608, 2006. 723, 724, 726, 741

Freitas, S. R., Longo, K. M., Chatfield, R., Latham, D., Silva Dias, M. A. F., Andreae, M. O., Prins, E., Santos, J. C., Gielow, R., and Carvalho Jr., J. A.: Including the sub-grid scale plume rise of vegetation fires in low resolution atmospheric transport models, *Atmos. Chem. Phys.*, 7, 3385–3398, doi:10.5194/acp-7-3385-2007, 2007. 724, 726, 727, 730, 731, 739, 741, 743, 744, 762

Freitas, S. R., Longo, K. M., Silva Dias, M. A. F., Chatfield, R., Silva Dias, P., Artaxo, P., Andreae, M. O., Grell, G., Rodrigues, L. F., Fazenda, A., and Panetta, J.: The Coupled Aerosol and Tracer Transport model to the Brazilian developments on the Regional Atmospheric Modeling System (CATT-BRAMS) – Part 1: Model description and evaluation, *Atmos. Chem. Phys.*, 9, 2843–2861, doi:10.5194/acp-9-2843-2009, 2009. 727, 734

Freitas, S. R., Longo, K. M., Trentmann, J., and Latham, D.: Technical Note: Sensitivity of 1-D smoke plume rise models to the inclusion of environmental wind drag, *Atmos. Chem. Phys.*, 10, 585–594, doi:10.5194/acp-10-585-2010, 2010. 724, 727, 728, 730, 731, 740, 741, 744, 749, 756, 759, 760, 761

Fromm, M., Bevilacqua, R., Servranckx, R., Rosen, J., Thayer, J. P., Herman, J., and Larko, D.: Pyro-cumulonimbus injection of smoke to the stratosphere: observations and impact of a

## One-dimensional simulation of fire injection heights

S. Strada et al.

Title Page

Abstract

Introduction

Conclusions

References

Tables

Figures

◀

▶

◀

▶

Back

Close

Full Screen / Esc

Printer-friendly Version

Interactive Discussion



super blowup in northwestern Canada on 3–4 August 1998, *J. Geophys. Res.*, 110, D08205, doi:10.1029/2004JD005350, 2005. 724

Gidel, L.: Cumulus cloud transport of transient tracers, *J. Geophys. Res.*, 88, 6587–6599, doi:10.1029/JC088iC11p06587, 1983. 723

5 Gonzi, S. and Palmer, P. I.: Vertical transport of surface fire emissions observed from space, *J. Geophys. Res.*, 115, 148–227, doi:10.1029/2009JD012053, 2010. 726, 760

Graf, H., Herzog, M., Oberhuber, J., and Textor, C.: Effect of environmental conditions on volcanic plume rise, *J. Geophys. Res.*, 104, D20, 24309–24320, doi:10.1029/1999JD900498, 1999. 724

10 Grell, G., Freitas, S. R., Stuefer, M., and Fast, J.: Inclusion of biomass burning in WRF-Chem: impact of wildfires on weather forecasts, *Atmos. Chem. Phys.*, 11, 5289–5303, doi:10.5194/acp-11-5289-2011, 2011. 727

Guan, H., Chatfield, R. B., Freitas, S. R., Bergstrom, R. W., and Longo, K. M.: Modeling the effect of plume-rise on the transport of carbon monoxide over Africa with NCAR CAM, *Atmos. Chem. Phys.*, 8, 6801–6812, doi:10.5194/acp-8-6801-2008, 2008. 726

15 Guan, H., Esswein, R., Lopez, J., Bergstrom, R., Warnock, A., Follette-Cook, M., Fromm, M., and Iraci, L. T.: A multi-decadal history of biomass burning plume heights identified using aerosol index measurements, *Atmos. Chem. Phys.*, 10, 6461–6469, doi:10.5194/acp-10-6461-2010, 2010. 726, 760

20 Hodzic, A., Madronich, S., Bohn, B., Massie, S., Menut, L., and Wiedinmyer, C.: Wildfire particulate matter in Europe during summer 2003: meso-scale modeling of smoke emissions, transport and radiative effects, *Atmos. Chem. Phys.*, 7, 4043–4064, doi:10.5194/acp-7-4043-2007, 2007. 726, 734, 760

Honnert, R., Masson, V., and Couvreux, F.: A diagnostic for evaluating the representation of turbulence in atmospheric models at the kilometric scale, *J. Atmos. Sci.*, 68, 3112–3131, doi:10.1175/JAS-D-11-061.1, 2011. 759, 761

25 Hourdin, F., Couvreux, F., and Menut, L.: Parameterization of the dry convective boundary layer based on a mass flux representation of thermals, *J. Atmos. Sci.*, 59, 1105–1123, 2002. 727, 736, 737

30 Hyer, E. J., Allen, D. J., and Kasischke, E. S.: Examining injection properties of boreal forest fires using surface and satellite measurements of CO transport, *J. Geophys. Res.*, 112, 148–227, doi:10.1029/2006JD008232, 2007. 726

## One-dimensional simulation of fire injection heights

S. Strada et al.

Title Page

Abstract

Introduction

Conclusions

References

Tables

Figures

◀

▶

◀

▶

Back

Close

Full Screen / Esc

Printer-friendly Version

Interactive Discussion



Kahn, R. A., Chen, Y., Nelson, D. L., Leung, F.-Y., Li, Q., Diner, D. J., and Logan, J. A.: Wildfire smoke injection heights: two perspectives from space, *Geophys. Res. Lett.*, 35, 4, doi:10.1029/2007GL032165, 2008. 723, 725

Kain, J. and Fritsch, J.: A one-dimensional entraining/detraining plume model and its application in convective parameterization, *J. Atmos. Sci.*, 47, 2784–2802, 1990. 738

Kaiser, J. W., Heil, A., Andreae, M. O., Benedetti, A., Chubarova, N., Jones, L., Morcrette, J.-J., Razinger, M., Schultz, M. G., Suttie, M., and van der Werf, G. R.: Biomass burning emissions estimated with a global fire assimilation system based on observed fire radiative power, *Biogeosciences*, 9, 527–554, doi:10.5194/bg-9-527-2012, 2012. 762

Labonne, M. and Chevallier, F.-M. B. F.: Injection height of biomass burning aerosols as seen from a spaceborne, *Geophys. Res. Lett.*, 34, 11806–11811, 2007. 725, 760

Lafore, J. P., Stein, J., Asencio, N., Bougeault, P., Ducrocq, V., Duron, J., Fischer, C., Héreil, P., Mascart, P., Masson, V., Pinty, J. P., Redelsperger, J. L., Richard, E., and Vilà-Guerau de Arellano, J.: The Meso-NH Atmospheric Simulation System. Part I: adiabatic formulation and control simulations, *Ann. Geophys.*, 16, 90–109, doi:10.1007/s00585-997-0090-6, 1998. 733

Lamarque, J.-F., Edwards, D. P., Emmons, L. K., Gille, J. C., Wilhelmi, O., Gerbig, C., Prevedel, D., Deeter, M. N., Warner, J., Ziskin, D. C., Khattatov, B., Francis, G. L., Yudin, V., Ho, S., Mao, D., Chen, J., and Drummond, J. R.: Identification of CO plumes from MOPITT data: application to the August 2000 Idaho-Montana forest fires, *J. Geophys. Res.*, 30, 13, 21-1, 1688, doi:10.1029/2003GL017503, 2003. 726

Latham, D.: A one-dimensional plume predictor and cloud model for fire and smoke managers, in: General Technical Report INT-GTR-314, USDA Forest Service, 305–312, 1994. 741

Lavoué, D., Liousse, C., Cachier, H., Stocks, B. J., and Goldammer, J. G.: Modeling of carbonaceous particles emitted by boreal and temperate wildfires at northern latitudes, *J. Geophys. Res.*, 105, 26871–26890, 2000. 726

Liousse, C., Penner, J. E., Chuang, C., Walton, J. J., Eddleman, H., and Cachier, H.: A global three-dimensional model study of carbonaceous aerosols, *J. Geophys. Res.*, 101, 19411–19432, doi:10.1029/95JD03426, 1996. 726

Longo, K. M., Freitas, S. R., Andreae, M. O., Setzer, A., Prins, E., and Artaxo, P.: The Coupled Aerosol and Tracer Transport model to the Brazilian developments on the Regional Atmospheric Modeling System (CATT-BRAMS) – Part 2: Model sensitivity to the biomass burning inventories, *Atmos. Chem. Phys.*, 10, 5785–5795, doi:10.5194/acp-10-5785-2010, 2010. 727

## One-dimensional simulation of fire injection heights

S. Strada et al.

Title Page

Abstract

Introduction

Conclusions

References

Tables

Figures

◀

▶

◀

▶

Back

Close

Full Screen / Esc

Printer-friendly Version

Interactive Discussion



- Lovejoy, T. E.: Global Biomass Burning: Atmospheric, Climatic, and Biospheric Implications, chap. 9, 77–82, edited by: Levine, J. S., Cambridge, MA, 1991. 730
- Luderer, G., Trentmann, J., Winterrath, T., Textor, C., Herzog, M., Graf, H. F., and Andreae, M. O.: Modeling of biomass smoke injection into the lower stratosphere by a large forest fire (Part II): sensitivity studies, *Atmos. Chem. Phys.*, 6, 5261–5277, doi:10.5194/acp-6-5261-2006, 2006. 724, 741
- Luderer, G., Trentmann, J., and Andreae, M. O.: A new look at the role of fire-released moisture on the dynamics of atmospheric pyro-convection, *Int. J. Wildland Fire*, 18, 554–562, 2009. 746, 758
- Martin, D., Webber, D. M., Jones, S. J., Underwood, B. Y., Tickle, G. A., and Ramsdale, S. A.: Near- and intermediate-field dispersion from strongly buoyant sources, Final Report AEAT/1388, Warrington, 1997. 727
- Mazzoni, D., Logan, J. A., Diner, D., Kahn, R., Tong, L., and Li, Q.: A data-mining approach to associating MISR smoke plume heights with MODIS fire measurements, *Remote Sens. Environ.*, 107, 138–148, doi:10.1016/j.rse.2006.08.014, 2007. 725
- McCarter, R. and Broido, A.: Radiative and convective energy from wood crib fires, *Pyrodynamics*, 2, 65–85, 1965. 740
- Miranda, A. I.: An integrated numerical system to estimate air quality effects of forest fires, *Int. J. of Wildland Fire*, 13, 217–226, 2004. 726, 760
- Miranda, A. I., Monteiro, A., Martins, V., Carvalho, A., Schaap, M., Builtjes, P., and Borrego, C.: Forest fire impact on air quality over Portugal, in: *Air Pollution Modeling and Its Application XIX*, edited by: Borrego, C. and Miranda, A. I., NATO Science for Peace and Security Series C: Environmental Security, 190–198, Springer, Netherlands, 2008. 740, 741
- Morton, B. R., Taylor, G., and Turner, J. S.: Turbulent gravitational convection from maintained and instantaneous sources, *P. Roy. Soc. Lond. A. Mat.*, 234, 1–23, doi:10.1098/rspa.1956.0011, 1956. 742
- Noilhan, J. and Planton, S.: A simple parameterization of land surface processes for meteorological models, *Mon. Wea. Rev.*, 117, 536–549, 1989. 734
- Parmar, R. S., Welling, M., Andreae, M. O., and Helas, G.: Water vapor release from biomass combustion, *Atmos. Chem. Phys.*, 8, 6147–6153, doi:10.5194/acp-8-6147-2008, 2008. 724
- Pergaud, J., Masson, V., Malardel, S., and Couvreux, F.: A parameterization of dry thermals and shallow cumuli for mesoscale numerical weather prediction, *Bound.-Lay. Meteorol.*, 132, 83–106, 2009. 728, 736, 738, 760

## One-dimensional simulation of fire injection heights

S. Strada et al.

Title Page

Abstract

Introduction

Conclusions

References

Tables

Figures

◀

▶

◀

▶

Back

Close

Full Screen / Esc

Printer-friendly Version

Interactive Discussion



- Phuleria, H. C., Fine, P. M., Zhu, Y., and Sioutas, C.: Air quality impacts of the October 2003 Southern California wildfires, *J. Geophys. Res.*, 110, 148–227, 2005. 723
- Pinty, J. P. and Jabouille, P.: A mixed-phase cloud parameterization for use in mesoscale non-hydrostatic model: simulations of a squall line and of orographic precipitations, in: Proc. Conf. of Cloud Physics, Am. Meteorol. Soc., Everett, WA, USA, 217–220, 17–21 August 1998. 733
- Randall, D. A., Albrecht, B., Cox, S., Johnson, D., Minnis, P., Rossow, W., and Starr, D. O.: On fire at ten, *Adv. Geophys.*, 38, 37–128, 1996. 733
- Rio, C., Hourdin, F., and Chédin, A.: Numerical simulation of tropospheric injection of biomass burning products by pyro-thermal plumes, *Atmos. Chem. Phys.*, 10, 3463–3478, doi:10.5194/acp-10-3463-2010, 2010. 725, 727, 737, 759, 760
- Saarikoski, S., Sillanpää, M., Sofiev, M., Timonen, H., Saarnio, K., Teinilä, K., Karppinen, A., Kukkonen, J., and Hillamo, R.: Chemical composition of aerosols during a major biomass burning episode over northern Europe in spring 2006: experimental and modelling assessments, *Atmos. Environ.*, 41, 3577–3589, doi:10.1016/j.atmosenv.2006.12.053, 2007. 723
- Seiler, W. and Crutzen, P. J.: Estimates of gross and net fluxes of carbon between the biosphere and the atmosphere from biomass burning, *Clim. Change*, 2, 207–247, 1980. 740
- Sessions, W. R., Fuelberg, H. E., Kahn, R. A., and Winker, D. M.: An investigation of methods for injecting emissions from boreal wildfires using WRF-Chem during ARCTAS, *Atmos. Chem. Phys.*, 11, 5719–5744, doi:10.5194/acp-11-5719-2011, 2011. 727
- Siebesma, A. P. and Teixeira, J.: An advection-diffusion scheme for the convective boundary layer: description and 1d-results, in: Proc. 14th Symposium on Boundary Layers and Turbulence, 133–136, Amer. Met. Soc., Aspen, CO, USA, 7–11 August 2000. 736
- Silvani, X. and Morandini, F.: Fire spread experiments in the field: temperature and heat fluxes measurements, *Fire Safety J.*, 44, 279–285, 2009. 723, 741
- Simpson, J. and Wiggert, V.: Models of precipitating cumulus towers, *Mon. Wea. Rev.*, 97, 471–489, 1969. 737, 744
- Singh, H., Cai, C., Kaduwela, A., Weinheimer, A., and Wisthaler, A.: Interactions of fire emissions and urban pollution over California: ozone formation and air quality simulations, *Atmos. Environ.*, 56, 45–51, doi:10.1016/j.atmosenv.2012.03.046, 2012. 725, 760
- Sofiev, M., Siljamo, P., Karppinen, A., and Kukkonen, J.: Air quality forecasting during summer 2006: forest fires as one of major pollution sources in Europe, in: Air Pollution Modeling and Its Application XIX, edited by: Borrego, C. and Miranda, A. I., NATO Science for Peace and Security Series C: Environmental Security, 305–312, Springer, Netherlands, 2008. 723

## One-dimensional simulation of fire injection heights

S. Strada et al.

Title Page

Abstract

Introduction

Conclusions

References

Tables

Figures

◀

▶

◀

▶

Back

Close

Full Screen / Esc

Printer-friendly Version

Interactive Discussion



Sofiev, M., Vankevich, R., Lotjonen, M., Prank, M., Petukhov, V., Ermakova, T., Koskinen, J., and Kukkonen, J.: An operational system for the assimilation of the satellite information on wild-land fires for the needs of air quality modelling and forecasting, *Atmos. Chem. Phys.*, 9, 6833–6847, doi:10.5194/acp-9-6833-2009, 2009. 726

5 Sofiev, M., Ermakova, T., and Vankevich, R.: Evaluation of the smoke-injection height from wild-land fires using remote-sensing data, *Atmos. Chem. Phys.*, 12, 1995–2006, doi:10.5194/acp-12-1995-2012, 2012. 723, 727, 758, 760

Stein, A. F., Rolph, G. D., Draxler, R. R., Stunder, B., and Ruminski, M.: Verification of the NOAA smoke forecasting system: model sensitivity to the injection height, *Wea. Forecasting*, 24, 379–394, doi:10.1175/2008WAF2222166.1, 2009. 723

10 Strada, S., Mari, C., Filippi, J. B., and Bosseur, F.: Wildfire and the atmosphere: modelling the chemical and dynamic interactions at the regional scale, *Atmos. Environ.*, 51, 234–249, doi:10.1016/j.atmosenv.2012.01.023, 2012. 730, 739, 740, 741, 752, 758, 759, 761

Trelles, J., Mcgrattan, K., and Baum, H.: Smoke transport by sheared winds, *Combust. Theor. Model.*, 3, 323–341, 1999. 730

15 Trentmann, J., Andreae, M. O., and Graf, H.-F.: Chemical processes in a young biomass-burning plume, *J. Geophys. Res.*, 108, 4705, doi:10.1029/2003JD003732, 2003. 750, 762

Trentmann, J., Luderer, G., Winterrath, T., Fromm, M. D., Servranckx, R., Textor, C., Herzog, M., Graf, H.-F., and Andreae, M. O.: Modeling of biomass smoke injection into the lower strato-  
20 sphere by a large forest fire (Part I): reference simulation, *Atmos. Chem. Phys.*, 6, 5247–5260, doi:10.5194/acp-6-5247-2006, 2006. 724

Tressol, M., Ordonez, C., Zbinden, R., Brioude, J., Thouret, V., Mari, C., Nedelec, P., Cam-  
25 mas, J.-P., Smit, H., Patz, H.-W., and Volz-Thomas, A.: Air pollution during the 2003 Eu-  
ropean heat wave as seen by MOZAIC airliners, *Atmos. Chem. Phys.*, 8, 2133–2150,  
doi:10.5194/acp-8-2133-2008, 2008. 724, 726

Turquety, S., Hurtmans, D., Hadji-Lazaro, J., Coheur, P.-F., Clerbaux, C., Josset, D., and  
Tsamalis, C.: Tracking the emission and transport of pollution from wildfires using the IASI  
CO retrievals: analysis of the summer 2007 Greek fires, *Atmos. Chem. Phys.*, 9, 4897–4913,  
doi:10.5194/acp-9-4897-2009, 2009. 723

30 Val Martin, M., Logan, J. A., Kahn, R. A., Leung, F.-Y., Nelson, D. L., and Diner, D. J.: Smoke  
injection heights from fires in North America: analysis of 5 years of satellite observations,  
*Atmos. Chem. Phys.*, 10, 1491–1510, doi:10.5194/acp-10-1491-2010, 2010. 725, 726, 760

- ValMartin, M., Kahn, R. A., Logan, J. A., Paugam, R., Wooster, M., and Ichoku, C.: Space-based observational constraints for 1-D fire smoke plume-rise models, *J. Geophys. Res.*, 117, D22204, doi:10.1029/2012JD018370, 2012. 762
- 5 Witek, M. L., Teixeira, J., and Matheou, G.: An eddy-diffusivity/mass-flux approach to the vertical transport of turbulent kinetic energy in convective boundary layers, *J. Atmos. Sci.*, 68, 10, 2385–2394, doi:10.1175/JAS-D-11-06.1, in press, 2011. 736
- Wyngaard, J. C.: Toward numerical modeling in the “Terra Incognita”, *J. Atmos. Sci.*, 61, 1816–1826, 2004. 759, 761

# GMDD

6, 721–790, 2013

## One-dimensional simulation of fire injection heights

S. Strada et al.

Title Page

Abstract

Introduction

Conclusions

References

Tables

Figures

⏪

⏩

◀

▶

Back

Close

Full Screen / Esc

Printer-friendly Version

Interactive Discussion





## One-dimensional simulation of fire injection heights

S. Strada et al.

**Table 2.** Environmental and updraft variables selected in the Meso-NH and Plume Rise models for discussing the simulation results.

Variables	Meso-NH		PRM
	Grid	Updraft	
Water vapour mixing ratio ( $\text{g kg}^{-1}$ )	$r_v$		$r_{v,f}$
Vertical velocity ( $\text{m s}^{-1}$ )		$w_u$	$w_f$
Buoyancy ( $\text{m s}^{-2}$ )		$B_u$	$B_f$
Turbulent heat flux ( $\text{K m s}^{-1}$ )		$\langle w'_u \theta'_u \rangle$	
Turbulent moist flux ( $\text{kg kg}^{-1} \text{m s}^{-1}$ )		$\langle w'_u r'_{v,u} \rangle$	
Turbulent kinetic energy ( $\text{m}^2 \text{s}^{-2}$ )	TKE		
Lateral entrainment rate ( $\text{s}^{-1}$ )		$\varepsilon_u$	$\varepsilon_{f,lat}$
Dynamic entrainment rate ( $\text{s}^{-1}$ )			$\varepsilon_{f,dyn}$
Detrainment rate ( $\text{s}^{-1}$ )		$\delta_u$	
Injection layer		$[\varepsilon_u]_{\max}$	VMD (%)
Normalized scalar mixing ratio	$r_s$		

Title Page

Abstract

Introduction

Conclusions

References

Tables

Figures

◀

▶

◀

▶

Back

Close

Full Screen / Esc

Printer-friendly Version

Interactive Discussion



## One-dimensional simulation of fire injection heights

S. Strada et al.

**Table 3.** Summary of numerical experiments that were performed with the 1-D models (Meso-NH and Plume Rise Model) and discussed in the present study.

Fire episode	Atmospheric forcing	Meso-NH		PRM
		TURB	EDMF	Environmental wind effect
Lançon 2005	RSOU	On	On	On
	ECMWF	On	Off	On
Rondônia 2002	Calm-dry	RSOU	On	On
		ECMWF	On	On
	Windy-wet	RSOU	On	On
		ECMWF	On	On

Title Page

Abstract

Introduction

Conclusions

References

Tables

Figures

⏪

⏩

◀

▶

Back

Close

Full Screen / Esc

Printer-friendly Version

Interactive Discussion



## One-dimensional simulation of fire injection heights

S. Strada et al.

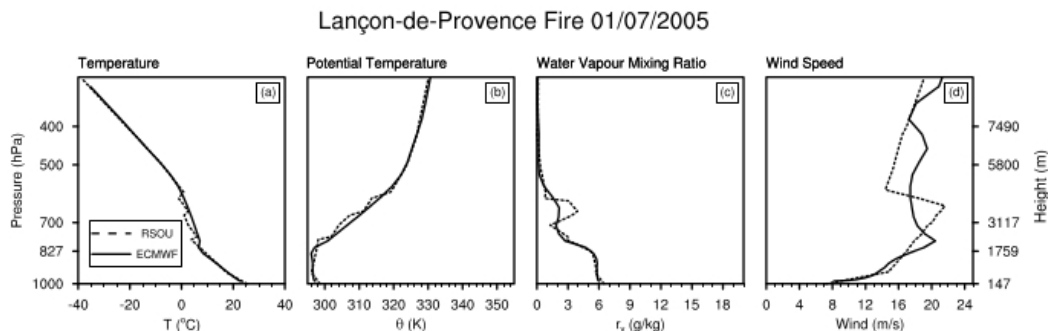


**Fig. 1.** Comparison between the radiosonde data (dashed line) and the analyses from the European Center for Meteorological and Weather Forecasting (solid line) for the Lançon-de-Provence 2005. The four graphics represent the vertical profile of: **(a)** temperature  $T$  ( $^{\circ}\text{C}$ ), **(b)** potential temperature  $\theta$  (K), **(c)** water vapour mixing ratio  $r_v$  ( $\text{g kg}^{-1}$ ) and **(d)** wind speed ( $\text{ms}^{-1}$ ).

Title Page

Abstract

Introduction

Conclusions

References

Tables

Figures

◀

▶

◀

▶

Back

Close

Full Screen / Esc

Printer-friendly Version

Interactive Discussion



## One-dimensional simulation of fire injection heights

S. Strada et al.

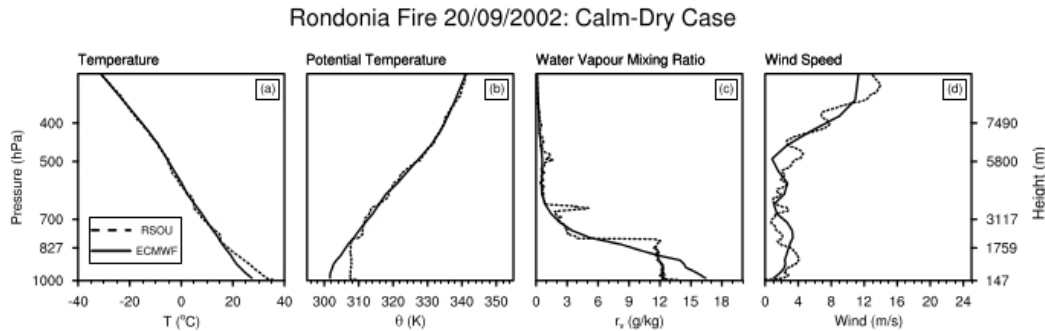


**Fig. 2.** The same as Fig. 1 for the calm-dry case of Rondônia 2002.

Title Page

Abstract

Introduction

Conclusions

References

Tables

Figures



Back

Close

Full Screen / Esc

Printer-friendly Version

Interactive Discussion



## One-dimensional simulation of fire injection heights

S. Strada et al.

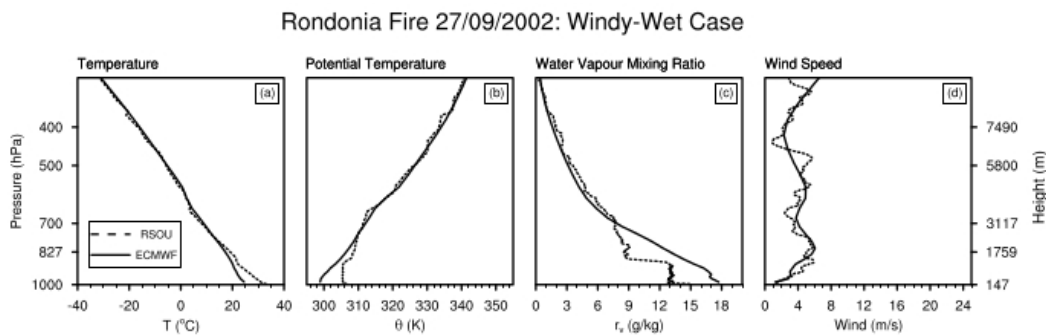


**Fig. 3.** The same as Fig. 1 for the windy-wet case of Rondônia 2002.

Title Page

Abstract

Introduction

Conclusions

References

Tables

Figures

◀

▶

◀

▶

Back

Close

Full Screen / Esc

Printer-friendly Version

Interactive Discussion



## One-dimensional simulation of fire injection heights

S. Strada et al.

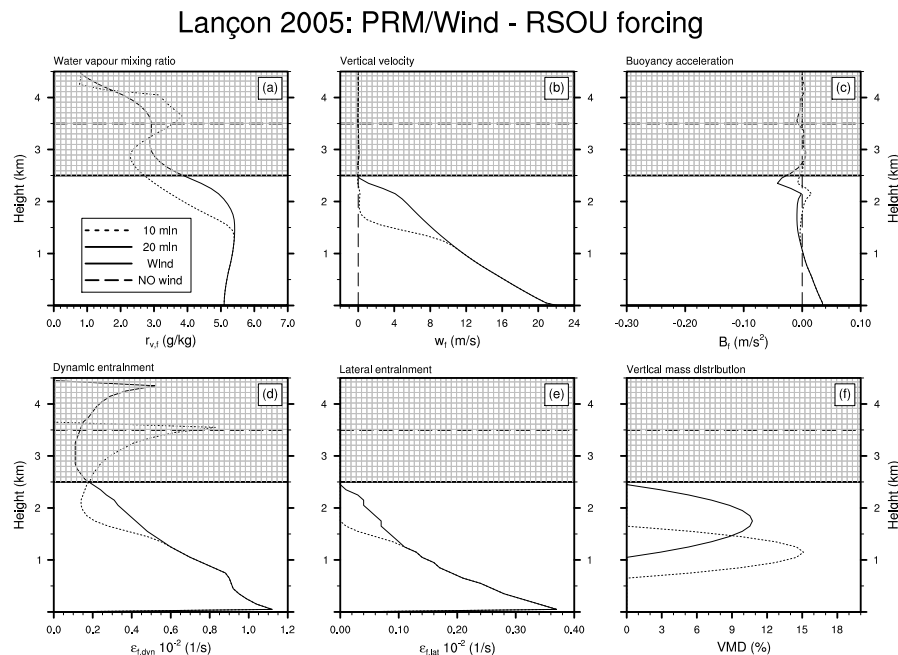


**Fig. 4.** 1-D Plume Rise Model results for the Lançon fire using the radiosounding of Nîmes as meteorological forcing. The quantities are: **(a)** water vapour mixing ratio ( $r_{v,f}$ ,  $\text{g kg}^{-1}$ ); **(b)** vertical velocity ( $w_f$ ,  $\text{m s}^{-1}$ ); **(c)** buoyancy acceleration ( $B_f$ ,  $\text{m s}^{-2}$ ); **(d)** dynamic entrainment ( $\epsilon_{f,\text{dyn}}$ ,  $\text{s}^{-1}$ ); **(e)** lateral entrainment ( $\epsilon_{f,\text{lat}}$ ,  $\text{s}^{-1}$ ); **(f)** vertical mass distribution (VMD, %). The solid line indicates the plume top obtained including the environmental wind effect; the horizontal dashed line is the plume top when the wind effect is off.

Title Page

Abstract

Introduction

Conclusions

References

Tables

Figures

◀

▶

◀

▶

Back

Close

Full Screen / Esc

Printer-friendly Version

Interactive Discussion



## One-dimensional simulation of fire injection heights

S. Strada et al.

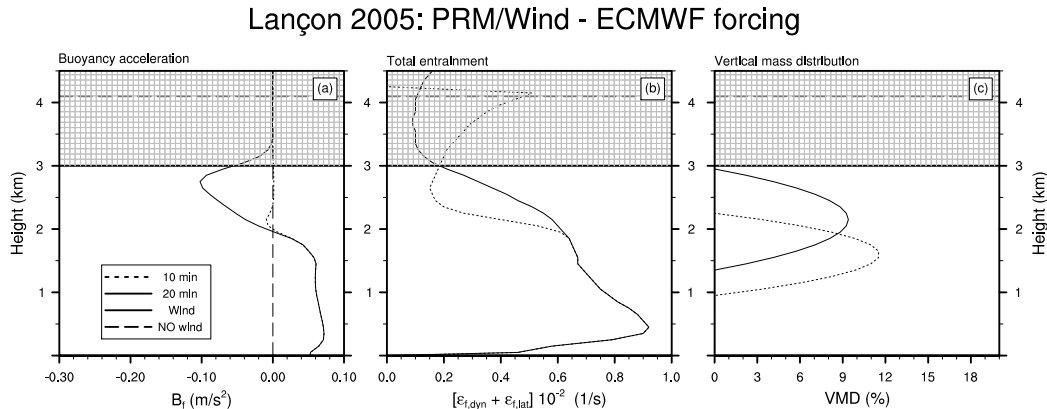


**Fig. 5.** 1-D Plume Rise Model results for the Lançon fire using the ECMWF re-analyses as meteorological forcing. The quantities are: **(a)** buoyancy acceleration ( $B_f$ ,  $\text{ms}^{-2}$ ); **(b)** total entrainment ( $\varepsilon_{f,\text{dyn}} + \varepsilon_{f,\text{lat}}$ ,  $\text{s}^{-1}$ ); **(c)** vertical mass distribution (VMD, %). The solid line indicates the plume top obtained including the environmental wind effect; the horizontal dashed line is the plume top when the wind effect is off.

Title Page

Abstract

Introduction

Conclusions

References

Tables

Figures

◀

▶

◀

▶

Back

Close

Full Screen / Esc

Printer-friendly Version

Interactive Discussion



One-dimensional simulation of fire injection heights

S. Strada et al.

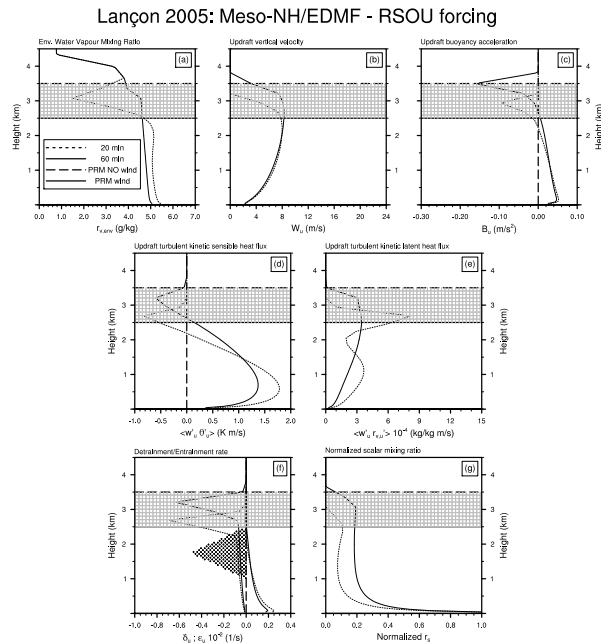


**Fig. 6.** 1-D Meso-NH/Eddy Diffusivity–Mass Flux results for the Lançon fire using the radiosounding of Nîmes as meteorological forcing. The quantities are: **(a)** environmental water vapour mixing ratio ( $r_{v,env}$ ,  $\text{gkg}^{-1}$ ); **(b)** updraft vertical velocity ( $w_u$ ,  $\text{ms}^{-1}$ ); **(c)** updraft buoyancy acceleration ( $B_u$ ,  $\text{ms}^{-2}$ ); **(d)** updraft turbulent kinetic sensible heat flux ( $\langle w'_u \theta'_u \rangle$ ,  $\text{Kms}^{-1}$ ); **(e)** updraft turbulent kinetic latent heat flux ( $\langle w'_u r'_{v,u} \rangle$ ,  $\text{kgkg}^{-1} \text{ms}^{-1}$ ); **(f)** detrainment rate when values are negative ( $\delta_u$ ,  $\text{s}^{-1}$ ), entrainment rate for positive values ( $\epsilon_u$ ,  $\text{s}^{-1}$ ); **(g)** normalized scalar flux. The horizontal solid (dashed) line is the plume top obtained with the environmental wind effect on (off) in the respective 1-D Plume Rise Model simulation. The dot filled area indicates where the VMD has positive values.

## One-dimensional simulation of fire injection heights

S. Strada et al.

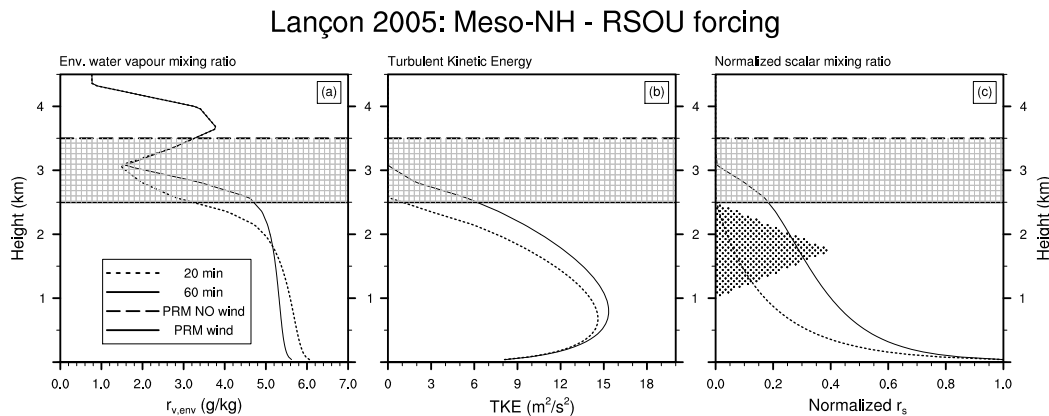


**Fig. 7.** 1-D Meso-NH results for the Lançon fire using the radiosounding of Nîmes as meteorological forcing, without activating the Eddy Diffusivity–Mass Flux scheme. The quantities are only referred to the environment: **(a)** environmental water vapour mixing ratio ( $r_{v,env}$ ,  $\text{g kg}^{-1}$ ); **(b)** turbulent kinetic energy (TKE,  $\text{m}^2 \text{s}^{-2}$ ); **(c)** normalized scalar mixing ratio. The horizontal solid (dashed) line is the plume top obtained with the environmental wind effect on (off) in the respective 1-D Plume Rise Model simulation. The dot filled area indicates where the VMD has positive values.

## One-dimensional simulation of fire injection heights

S. Strada et al.

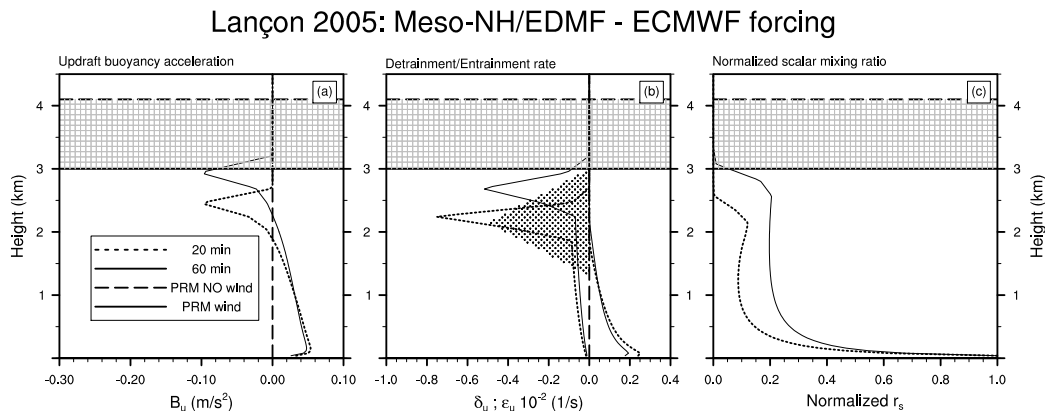


**Fig. 8.** 1-D Meso-NH/Eddy Diffusivity–Mass Flux results for the Lançon fire using the ECMWF re-analyses as meteorological forcing. The quantities are: **(a)** updraft buoyancy acceleration ( $B_u$ ,  $\text{m s}^{-2}$ ); **(b)** detrainment rate when values are negative ( $\delta_u$ ,  $\text{s}^{-1}$ ), entrainment rate for positive values ( $\epsilon_u$ ,  $\text{s}^{-1}$ ); **(c)** normalized scalar mixing ratio. The horizontal solid (dashed) line is the plume top obtained with the environmental wind effect on (off) in the respective 1-D Plume Rise Model simulation. The dot filled area indicates where the VMD has positive values.

## One-dimensional simulation of fire injection heights

S. Strada et al.

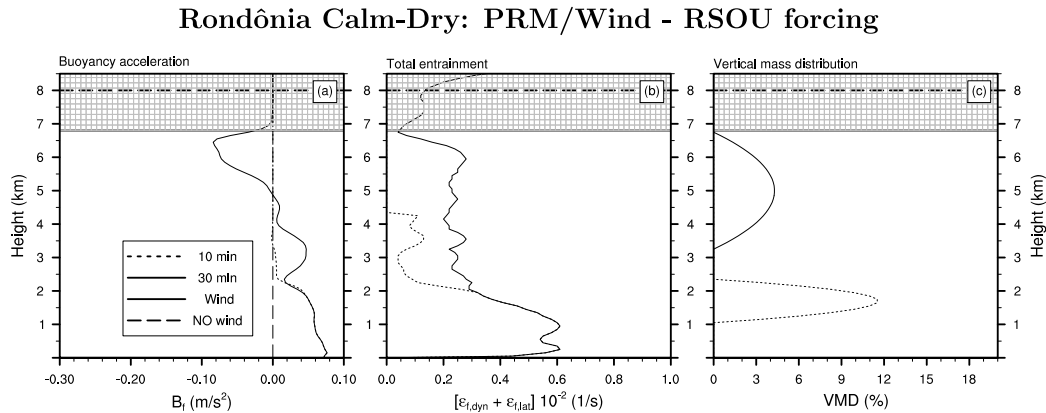


**Fig. 9.** The same as Fig. 5 for the calm-dry case of Rondônia (20 September 2002) using the radiosounding as meteorological forcing.

Title Page

Abstract

Introduction

Conclusions

References

Tables

Figures

◀

▶

◀

▶

Back

Close

Full Screen / Esc

Printer-friendly Version

Interactive Discussion



One-dimensional  
simulation of fire  
injection heights

S. Strada et al.

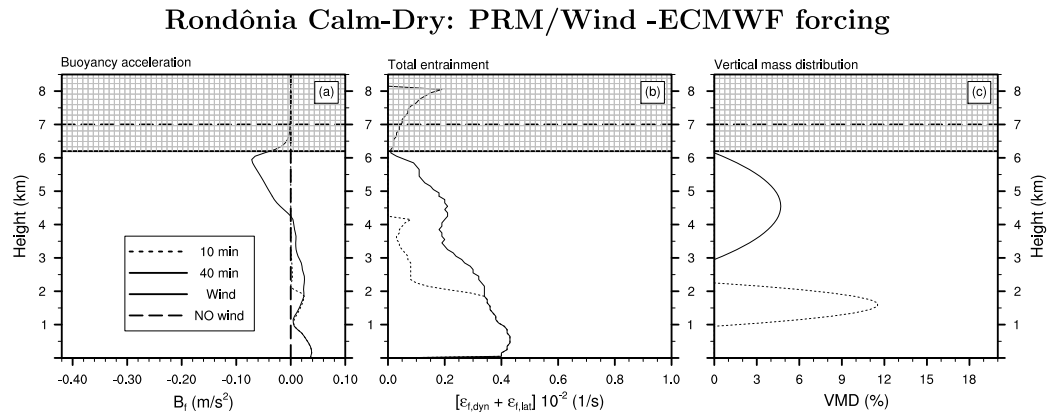


**Fig. 10.** The same as Fig. 5 for the calm-dry case of Rondônia (20 September 2002) using the ECMWF re-analyses as meteorological forcing.

Title Page

Abstract

Introduction

Conclusions

References

Tables

Figures

◀

▶

◀

▶

Back

Close

Full Screen / Esc

Printer-friendly Version

Interactive Discussion



## One-dimensional simulation of fire injection heights

S. Strada et al.

### Rondônia Calm-Dry: Meso-NH/EDMF - RSOU forcing

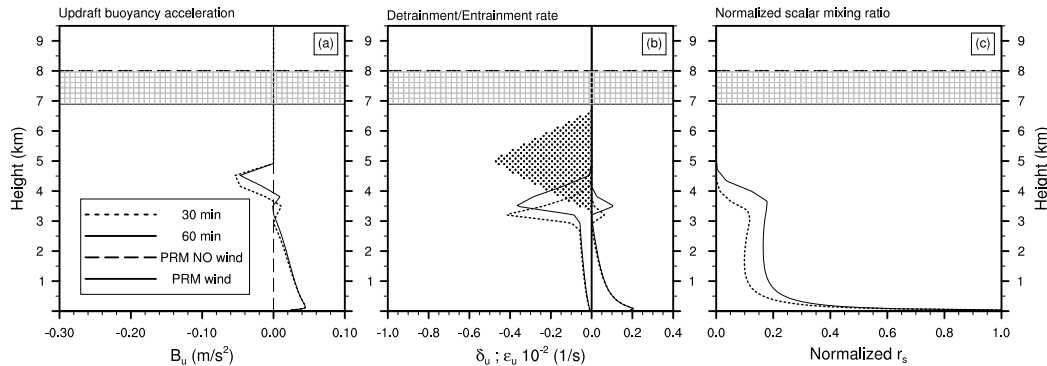


**Fig. 11.** The same as Fig. 8 for the calm-dry case of Rondônia (20 September 2002) using the radiosounding as meteorological forcing.

Title Page

Abstract

Introduction

Conclusions

References

Tables

Figures

◀

▶

◀

▶

Back

Close

Full Screen / Esc

Printer-friendly Version

Interactive Discussion



## One-dimensional simulation of fire injection heights

S. Strada et al.

### Rondônia Calm-Dry: Meso-NH/EDMF - ECMWF forcing

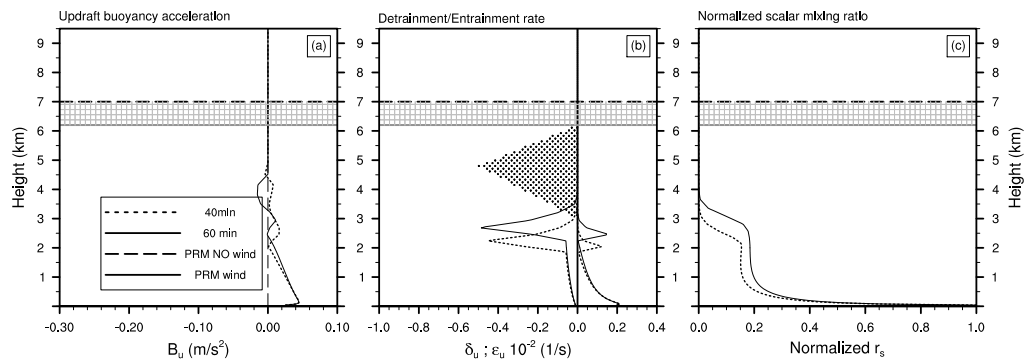


**Fig. 12.** The same as Fig. 8 for the calm-dry case of Rondônia fires (20 September 2002) using the ECMWF re-analyses as meteorological forcing.

Title Page

Abstract

Introduction

Conclusions

References

Tables

Figures



Back

Close

Full Screen / Esc

Printer-friendly Version

Interactive Discussion



## One-dimensional simulation of fire injection heights

S. Strada et al.

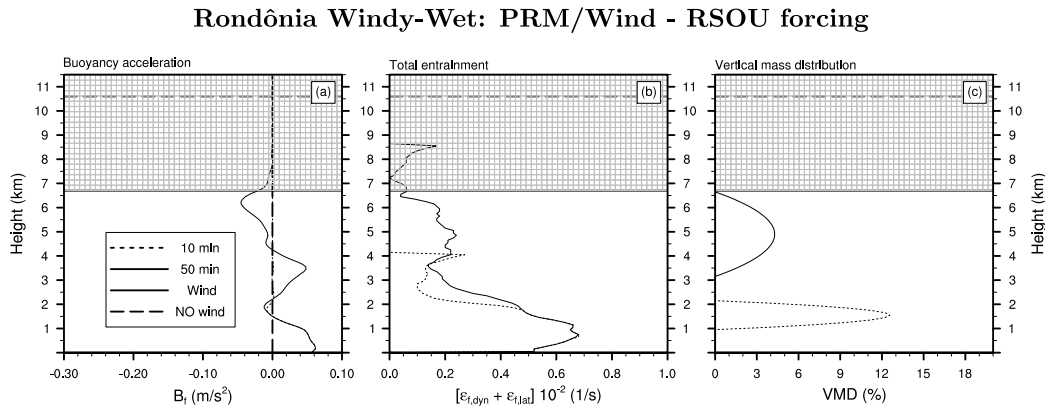


**Fig. 13.** The same as Fig. 5 for the windy-wet case of Rondônia fires (27 September 2002) using the radiosounding as meteorological forcing.

Title Page

Abstract

Introduction

Conclusions

References

Tables

Figures

◀

▶

◀

▶

Back

Close

Full Screen / Esc

Printer-friendly Version

Interactive Discussion



## One-dimensional simulation of fire injection heights

S. Strada et al.

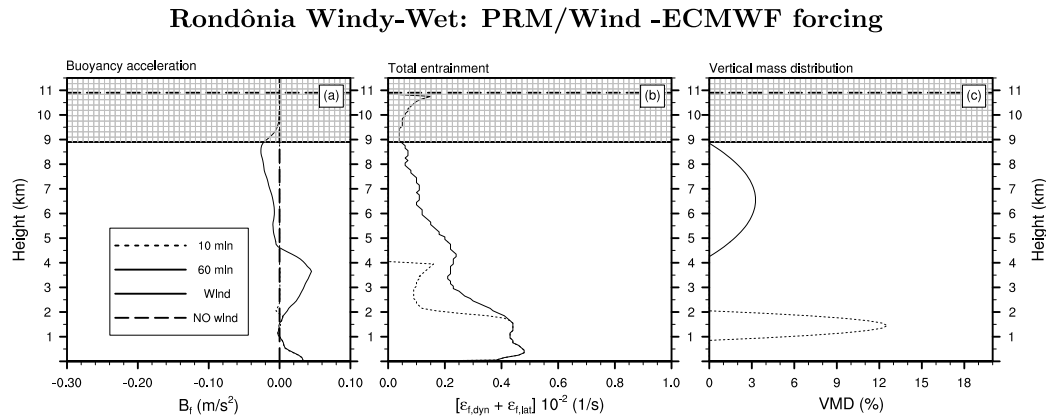


**Fig. 14.** The same as Fig. 5 for the windy-wet case of Rondônia fires (27 September 2002) using the ECMWF re-analyses as meteorological forcing.

Title Page

Abstract

Introduction

Conclusions

References

Tables

Figures

◀

▶

◀

▶

Back

Close

Full Screen / Esc

Printer-friendly Version

Interactive Discussion



**One-dimensional simulation of fire injection heights**

S. Strada et al.

**Rondônia Windy-Wet: Meso-NH/EDMF - RSOU forcing**

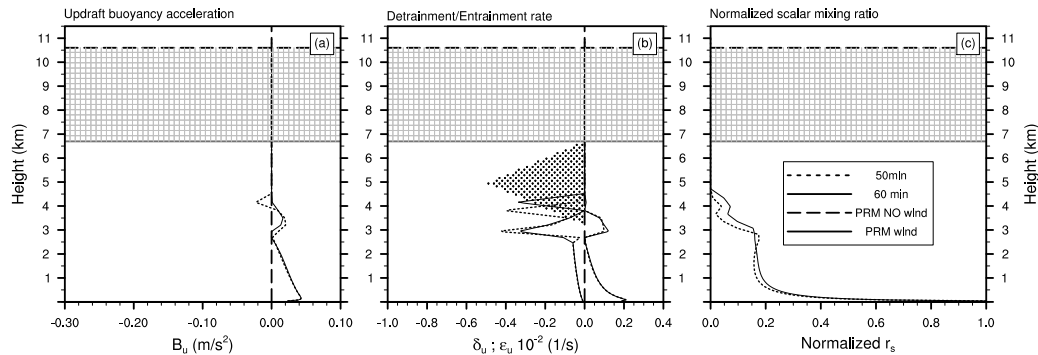


**Fig. 15.** The same as Fig. 8 for the windy-wet case of Rondônia fires (27 September 2002) using the radiosounding as meteorological forcing.

Title Page

Abstract

Introduction

Conclusions

References

Tables

Figures

⏪

⏩

◀

▶

Back

Close

Full Screen / Esc

Printer-friendly Version

Interactive Discussion



## One-dimensional simulation of fire injection heights

S. Strada et al.

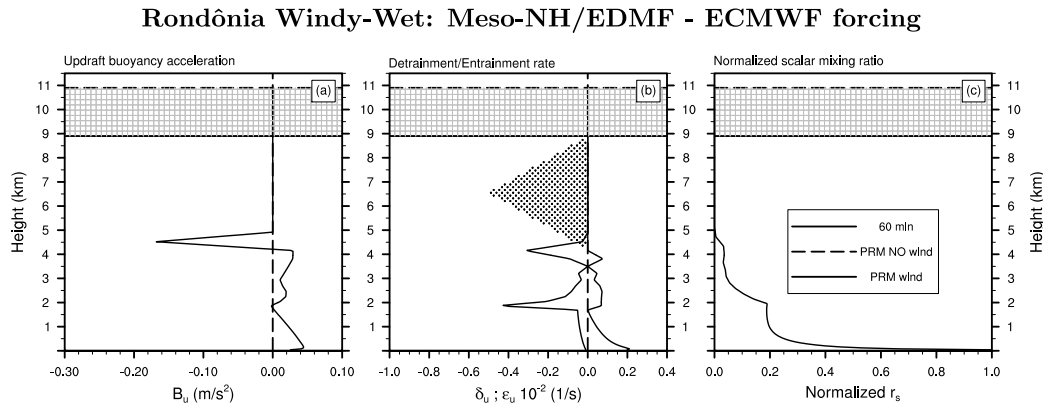


**Fig. 16.** The same as Fig. 8 for the windy-wet case of Rondônia fires (27 September 2002) using the ECMWF re-analyses as meteorological forcing.

Title Page

Abstract

Introduction

Conclusions

References

Tables

Figures

◀

▶

◀

▶

Back

Close

Full Screen / Esc

Printer-friendly Version

Interactive Discussion



## One-dimensional simulation of fire injection heights

S. Strada et al.

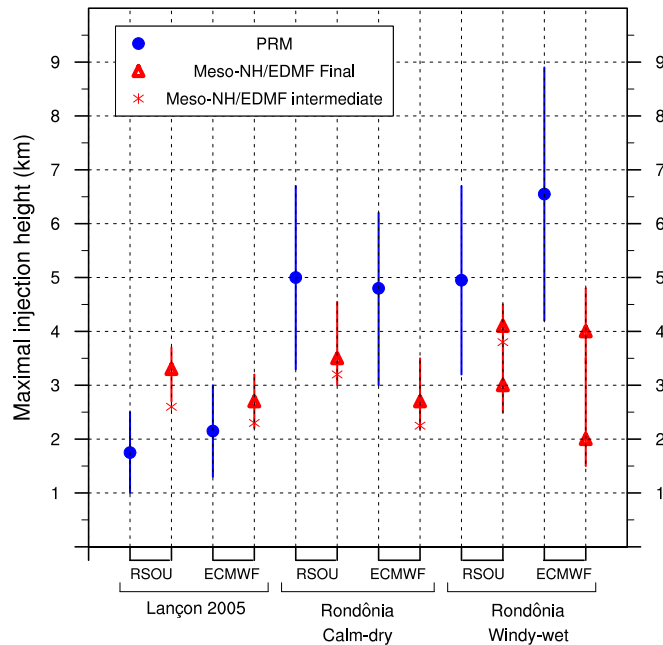


**Fig. 17.** Fire injection height and plume base and top as predicted by the two numerical models. For each of the three wild-fires, the two numerical forcings are distinguished: RSOU for the radiosonde, ECMWF for the re-analyses. The blue dots show the steady state solution attained by the PRM model, and they correspond to the level of maximum VMD with the associated width of the injection layer (blue error bar). The red triangles represent the final result given by the Meso-NH/EDMF model (after 60 min of simulation): they correspond to the level of maximum detrainment with the associated extent of the injection layer (red error bar). Red crosses are the intermediate results of the Meso-NH/EDMF model at the time of the steady state solution of the PRM model.

Title Page

Abstract

Introduction

Conclusions

References

Tables

Figures

◀

▶

◀

▶

Back

Close

Full Screen / Esc

Printer-friendly Version

Interactive Discussion

